Semicond. Sci. Technol. **15** (2000) R65–R80. Printed in the UK PII: S0268-1242(00)17828-9

TOPICAL REVIEW

Microscopic theory of exciton coherent control and Rayleigh scattering in semiconductor quantum wells

J Fernández-Rossier†§, C Tejedor† and R Merlin‡

† Departamento de Física Teórica de la Materia Condensada, Universidad Autónoma de Madrid, Cantoblanco, 28049 Madrid, Spain
‡ Department of Physics, The University of Michigan, Ann Arbor, MI 48109-1120, USA

Received 6 October 2000, accepted for publication 12 October 2000

Abstract. We present a bosonic description of excitons created by means of resonant optical pumping in a quantum well in the presence of a weak disorder potential. The excitonic collective state is a Glauber coherent state, closely related to that of photons but substantially different from that of few-level models. The theory, applying to the low-density regime, is used to explain various transient linear optical experiments involving resonantly excited excitons in GaAs quantum wells. In particular, we consider coherent control of the exciton density and spin, resonant Rayleigh scattering and scattering coherent control. Our quantum mechanical approach for light emission shows that excitonic secondary emission has a coherent component, in agreement with experiments.

(Some figures in this article are in colour only in the electronic version; see `www.iop.org`)

1. Introduction

The coherent response of GaAs quantum wells (QW) to ultrafast laser pulses has been the object of intense research in the last decade. More recently, the use of resonant, low-intensity subpicosecond pulses, at low temperatures, has provided a wealth of information on the exciton *linear response* [1–12]. In these 'linear' experiments‖, coherence is revealed by some interference phenomena which, broadly speaking, can be classified into three groups:

(i) *Temporal coherent control.* This refers to the case where a single excitonic resonance is driven by *two* identical laser pulses [2, 5, 6, 8] whose mutual delay, τ, can be controlled with atosecond precision. The main feature of coherent control is that some property of the system (e.g. the exciton density [2] or optical orientation [5]) is an oscillating function of τ. The amplitude of the oscillations goes to zero in a timescale referred to as T_2.

(ii) *Resonant Rayleigh scattering (RRS).* A QW excited by a laser pulse with in-plane momentum $\boldsymbol{k}_{||}$ emits coherent light [1, 3, 7, 8, 10–12] in non-phase-matched directions $\boldsymbol{q}_{||} \neq \boldsymbol{k}_{||}$. This is due to disorder, which breaks the translational invariance along the QW plane, producing elastic scattering events which preserve the phase coherence.

(iii) *Light–heavy hole exciton (lx–hx) beats*¶. These take place whenever the pulses overlap in energy with both the lx- and hx-states. Beats are observed, for instance, in the time resolved intensity of the RRS [1, 3, 7, 8, 11, 12] or in time resolved reflectivity [2, 3]. It must be noted that (i), (ii) and (iii) can all be observed simultaneously in the same experiment [8, 9].

Interferences do take place, but *what* is interfering? There are two apparently different possibilities: (i) interferences involving the induced electric dipole and (ii) quantum interferences of the exciton wavefunction. Each possibility is related to a different kind of theoretical picture. The first one relies on the classical picture in which an electric dipole linearly proportional to the exciting electric field of the laser is induced in the QW, considered as a dielectric [13, 14]. The induced macroscopic dipole emits radiation that decays in a typical time T_2 (usually much shorter than the radiative decay time T_1). The second possibility brings us to a microscopic picture in which the laser creates a quantum coherent superposition state of excitons that decays in the time T_2.

§ Present address: Physics Department, University of California at San Diego, 9500 Gilman Drive, La Jolla, CA 92093, USA.

‖ The term 'linear' refers to experiments for which the dominant features of the interference originate from linear response and the exciton density is low.

¶ One of the issues of this paper is to clarify whether the beats are due to electromagnetic or quantum interferences.

One of the goals of this paper is to provide an unambiguous description of excitonic coherence. With this in mind, we claim that *excitonic coherence*, as revealed by *linear* experiments, is a many-noninteracting-exciton phenomenon, exactly as optical coherence is a many- (noninteracting-) photon phenomenon [15]. In analogy with Glauber theory of photonic coherence, we present a description of excitonic coherence, in the presence of a weak disorder potential, in terms of a quantum field theory of excitons. It must be emphasized that our theory unifies the electromagnetic and quantum pictures mentioned earlier. In the limit of a high number of quanta, and under certain conditions, quantum fields behave classically, in the sense that their mean values are much larger than the fluctuations. In that situation electromagnetic (classical) interferences dominate. In the opposite limit (low number of quanta) the quantum behaviour becomes the norm.

Disorder plays a central role in the experiments and, in particular, in time-resolved Rayleigh scattering [1,3,4,8–12]. Here, the decay of the macroscopic dipole [1–12] correlates with the finite exciton linewidth [13, 16], which is partially due to the disorder. Our microscopic description is based on a second quantized Hamiltonian of noninteracting *bosonic* excitons in a weak disorder potential. The same Hamiltonian has been used in other papers of this field [17, 18].

Our main result is an expression for the *exact* collective wavefunction of the QW excitons created by arbitrary laser pulses in an arbitrary weak disorder potential in the low-density regime. This wavefunction is identical to Glauber's coherent state, as in the disorder free case [18]. This provides an unambiguous description of excitonic coherence, similar to that of Glauber theory [15]. While our solution assumes the knowledge of the single exciton wavefunction in the disorder potential, which is difficult to obtain, much can be learned without even solving the actual problem.

The structure of this paper is as follows. Section 2 begins with the motivation of the model of noninteracting bosonic excitons in a weak disorder potential. We present the Hamiltonian and give a definition of exciton coherence. Afterwards we obtain the exact exciton wavefunction when the QW is driven by a laser pulse both with and without disorder. At the end of section 2, we propose an analytical ansatz for the solution of the single exciton in a disorder potential, which is used in the following sections to obtain analytical results. In section 3 we discuss coherent control of the exciton density [2,5,8] in a single QW. Although most of the experiments have been performed in a multi-QW, the effect of inter-well coupling is not important [6] and will be ignored in this paper.

In section 4 we address recent Rayleigh scattering experiments [1, 3, 7, 8, 10–12], by considering a quantum theory of light emission from coherent excitons. We show that RRS has a coherent component that displays lx–hx beats. In section 5 we analyse coherent control experiments on optical orientation [5] in which the exciton spin degree of freedom is the parameter of interest and in section 6 we study the experiments on coherent control of the Rayleigh signal [8,9]. Section 7 is devoted to the question of dephasing and a detailed analysis of the experimental results. The main conclusions are given in section 8.

2. The bosonic model

2.1. Justification of the model

In this section, we describe excitons as noninteracting bosons in a disorder potential. It is important to emphasize that, even if we are interested only in the linear response, the complete description of the excited QW involves many-exciton wavefunctions. As recently discussed by Victor *et al* [19], the linear excitonic *susceptibility* is correctly calculated by removing from the Hilbert space all the states with more than one exciton. Hereafter we refer to this approximation as the 'one-exciton' approach. It must be noted that the number of excitons in an excited QW is much higher than unity even under low-excitation conditions. For instance, a pulsed laser with an average power of 1 μW and a repetition rate of 100 MHz creates $\sim$1000 excitons/pulse in a GaAs QW of width 10 nm. Therefore, the proper physical description of a QW requires the use of many-exciton states to obtain both the correct linear susceptibility, $\chi(1)$, *and* the exciton number, in contrast with the 'one-exciton' approach, in which only the former is correctly given.

We can consider excitons as bosons as long as their overlap is very small. A measure of the overlap is given by na^2 where n is the exciton density and a is the exciton Bohr radius. Both the interaction between excitons and deviations of excitonic operators from pure bosonic behaviour increase with increasing na^2 [20, 21]. In the experiments of interest, the estimated densities are below 10^{10} cm^{-2}, so $na^2 < 10^{-2}$ (in [8,9] the density is $<10^7$ cm^{-2} or $na^2 < 10^{-4}$). We also note that, in order to minimize the generation of free electron–hole pairs, the measurements use resonant excitation and low temperatures ($<$20 K). Thus, it is safe to consider a truncated Hilbert space limited to the sector of 1s excitons [22].

Another approximation of our model is that we assume a *weak disorder* potential, i.e. one that couples to the exciton centre of mass but does not perturb the component of the wavefunction associated with the relative coordinate [23]. This condition requires that (i) the localization length associated to the disorder potential be much bigger than a and (ii) that the disorder potential be much weaker than the exciton binding energy. The experimental linewidth of the exciton peak is $<$1 meV in the samples that have been studied. Since the width gives an upper limit to the strength of the disorder, it is clear that (ii) is well obeyed.

Following these considerations, our Hamiltonian is that of a gas of noninteracting two-dimensional bosons, in the presence of a static potential, and coupled to the electromagnetic field [17, 18]:

$$\hat{H} = \hat{H}_0 + \hat{U} + \hat{H}_{\rm rad} + \hat{H}_{\rm int}. \tag{1}$$

The free-exciton, kinetic energy term is

$$\hat{H}_0 = \sum_{\boldsymbol{k}_{||},\alpha,M} \hbar\omega_{\boldsymbol{k}_{||},\alpha} A^{\dagger}_{\boldsymbol{k}_{||},\alpha,M} A_{\boldsymbol{k}_{||},\alpha,M} \tag{2}$$

where $A^{\dagger}_{\boldsymbol{k}_{||},\alpha,M}$ creates a QW 1s exciton with in-plane centre of mass momentum $\boldsymbol{k}_{||}$, third component of the angular momentum M and valence band index $\alpha = L, H$. We only consider optically active $M = \pm 1$ and heavy-hole ($\alpha = H$)

or light-hole ($\alpha = L$) excitons in the lowest QW state. The single exciton energy is given by $\hbar\omega_{k,\alpha} = E_\alpha^g - \epsilon_\alpha + \frac{\hbar^2 k^2}{2m_\alpha}$, where E_α^g is the semiconductor gap and ϵ_α is the exciton binding energy. The *weak disorder* potential $\hat{U}$ is given by

$$\hat{U} = \sum_{\alpha, \boldsymbol{q}_{||}, \boldsymbol{p}_{||}} V_\alpha(\boldsymbol{q}_{||} - \boldsymbol{p}_{||})(A^\dagger_{\boldsymbol{q}_{||},\alpha} A_{\boldsymbol{p}_{||},\alpha} + \text{c.c.}). \tag{3}$$

This term describes elastic scattering of excitons [17, 18]. Note that $\hat{U}$ does not mix lx and hx (3). The energy of the free electromagnetic field is given in terms of photon operators $b_{k,\lambda}$ by

$$\hat{H}_{\text{rad}} = \sum_{\boldsymbol{k},\lambda} \hbar c|\boldsymbol{k}| b^\dagger_{\boldsymbol{k},\lambda} b_{\boldsymbol{k},\lambda} \tag{4}$$

where $\boldsymbol{k} = (\boldsymbol{k}_{||}, k_z)$ is the three-dimensional photon wavevector and λ is the polarization index. Finally, the light–matter interaction is given by

$$\hat{H}_{\text{int}} = -\int \hat{\boldsymbol{E}}(\boldsymbol{r}) \cdot \hat{\boldsymbol{P}}(\boldsymbol{r})\, \mathrm{d}V \tag{5}$$

where the electric field operator is

$$\begin{aligned}\hat{\boldsymbol{E}}(\boldsymbol{r}, t) &= \sum_{\boldsymbol{k}_{||},k_z,\lambda} \sqrt{\left(\frac{\hbar c|k|}{2\epsilon_0 V}\right)} \vec{\epsilon}_{k,\lambda} \mathrm{e}^{-\mathrm{i}\boldsymbol{k}\cdot\boldsymbol{r}} b_{k,\lambda} + \text{c.c.} \\ &= \sum_{\boldsymbol{k}_{||},k_z,\lambda} [\hat{\boldsymbol{E}}^{(-)}_{\boldsymbol{k}_{||},k_z,\lambda} + \hat{\boldsymbol{E}}^{(+)}_{\boldsymbol{k}_{||},k_z,\lambda}] \\ &= \hat{\boldsymbol{E}}^{(-)}(\boldsymbol{r}, t) + \hat{\boldsymbol{E}}^{(+)}(\boldsymbol{r}, t),\end{aligned} \tag{6}$$

where $\vec{\epsilon}_{(k),\lambda}$ is the polarization vector [24] and V is the volume of the three-dimensional box in which the modes of the field are defined. The polarization field, i.e. the electric dipole density $\hat{\boldsymbol{P}}(\boldsymbol{\rho}, z)$† vanishes outside the QW. If we neglect the spatial dependence along z, we have inside the QW

$$\hat{\boldsymbol{P}}(\boldsymbol{\rho}) = \sum_{\boldsymbol{k}_{||}} \hat{\boldsymbol{P}}^{(+)}_{\boldsymbol{k}_{||}} \mathrm{e}^{\mathrm{i}\boldsymbol{k}_{||}\cdot\vec{\boldsymbol{\rho}}} + \text{c.c.} \tag{7}$$

where

$$\hat{\boldsymbol{P}}^{(+)}_{\boldsymbol{k}_{||}} = \frac{1}{\sqrt{V_{\text{QW}}}} \sum_{\alpha,M} G_{\alpha,M} A^\dagger_{\boldsymbol{k}_{||},\alpha,M} \vec{\boldsymbol{u}}_M \tag{8}$$

$G_{\alpha,M}$ is the electric dipole matrix element [16], V_{QW} is the QW volume and $\vec{\boldsymbol{u}}_{\pm 1}$ are unitary vectors associated with the left and right circular polarizations. In the rotating wave approximation, the matter–light coupling can be written as

$$\hat{H}_{\text{int}} = -\sum_{\boldsymbol{k}_{||},k_z,\boldsymbol{\lambda}} (\hat{\boldsymbol{P}}^{(+)}_{\boldsymbol{k}_{||}} \cdot \hat{\boldsymbol{E}}^{(-)}_{\boldsymbol{k}_{||},k_z,\lambda} + \text{c.c.}). \tag{9}$$

We treat the laser field as a classical object [13, 14, 16–19, 23, 25]. This means that, when we consider the interaction between the laser and the excitons, the electric field operator is replaced by the classical modes $\boldsymbol{E}_{k,\lambda}$. This approximation is justified because the laser modes are coherent and macroscopically occupied [24]. Here we make the additional simplifying assumption that considers a laser beam that is perpendicular to the QW so that the only term that remains in the sum is $\boldsymbol{k}_{||} = \boldsymbol{0}_{||}$. With this, the light–matter coupling term becomes

$$\hat{H}^{\text{cl}}_{\text{int}} = -\sum_{k_z,\lambda} \boldsymbol{E}_{\boldsymbol{0}_{||},k_z,\lambda}(t) \cdot (\hat{\boldsymbol{P}}^{(+)}_{\boldsymbol{0}_{||}} + \text{c.c.}) \tag{10}$$

where $\boldsymbol{E}_{\boldsymbol{0}_{||},k_z,\lambda}(t)$ is now a c-number.

In contrast with the above description, to study light *emission* from the QW the light modes of arbitrary $\boldsymbol{k}$ will be treated using quantum mechanics because their occupation can be very small. These modes are initially empty but become occupied due to the recombination of the QW excitons [26]. For the emission process, we will show that the light is coherent, in the sense defined by Glauber [15,26].

2.2. Exciton coherence

We give now a phenomenological definition of exciton coherence. In our discussion, an excitonic mode is referred to as coherent whenever

$$\langle A_{\boldsymbol{k}_{||}} \rangle \neq 0 \qquad \langle A^\dagger_{\boldsymbol{k}_{||}} \rangle \neq 0. \tag{11}$$

Here $\langle\ \rangle$ is the expectation value evaluated either using the quantum state or the density matrix that describes the system. This definition has an immediate consequence: *the expectation value of the electric dipole operator is nonzero as long as the state of the system is coherent*. This situation is identical to the case of photons [15,27–29] and it is similar to that of a Bose condensate for which the expectation value of the operator that creates a particle is nonzero [26,30].

In the following, we calculate the dynamics of coherent excitons created with a resonant subpicosecond laser. We will ignore the interaction between excitons and other excitations of the solid, say, phonons, so that we can describe the excitons in terms of a wavefunction instead of a density matrix. We will show that the exact exciton state is a Glauber state, also known as the *coherent state*. Such a state satisfies the criterion for coherence (11). To avoid confusion, we will refer to (11) as coherence 'in the broad sense'.

2.3. Exact solution of the model without disorder

We first solve the model (1) in the case $\hat{U} = 0$, i.e. for a perfect QW without disorder [18]. We do this because we want to compare the case with and without disorder and also to discuss the effect of disorder on the linear transient behaviour of the QW. To calculate the collective state of the excitons created by the laser, we neglect the quantum fluctuations of the electromagnetic field and assume that $E(t)$ is a prescribed function. As mentioned earlier, we will abandon this approximation to calculate the light *emitted* by the excitons.

For $\hat{U} = 0$, we have a perfect crystal driven by an external field. Defining $\sum_{k_z,\lambda} \boldsymbol{E}_{\boldsymbol{0}_{||},k_z,\lambda}(t) = \sum_M E_{\boldsymbol{0}_{||},M}(t)\vec{\boldsymbol{u}}_M$, we have

$$\begin{aligned}\hat{H}_{PC} &= \hat{H}_0 + \sqrt{V_{\text{QW}}} \\ &\quad \times \sum_{\alpha,M} E_{\boldsymbol{0}_{||},M}(t) G_{\alpha,M}(A^\dagger_{\boldsymbol{0}_{||},\alpha,M} + A_{\boldsymbol{0}_{||},\alpha,M}).\end{aligned} \tag{12}$$

† We refer to $\hat{\boldsymbol{P}}(\boldsymbol{\rho}, z)$ as the 'electric dipole' instead of the more standard 'polarization' or the longer 'electric-dipole density'. In this paper, 'polarization' is always used to refer to the vector character of the electromagnetic field.

Here, the presence of the factor $\sqrt{V_{\rm QW}}$ should be emphasized, for it is the factor that prevents us from applying perturbative approaches to calculate the wavefunction. $\hat{H}_{PC}$ describes a set of independent harmonic oscillators (the excitonic modes) that are driven linearly by a classical field. This problem can be solved *exactly*. Assuming that at $t = -\infty$ all the excitonic modes are empty [31] and the result is [18]

$$|\Xi\rangle = C\mathrm{e}^{-\mathrm{i}H_0 t/\hbar}\prod_{\alpha,M}\mathrm{e}^{\mathrm{i}K_{\mathbf{0}_{||},\alpha,M}(t)A^{\dagger}_{\mathbf{0}_{||},\alpha,M}}|0\rangle \tag{13}$$

where $C = \prod_{\alpha,M}\mathrm{e}^{-|K_{\mathbf{0}_{||},\alpha,M}|^2/2}$ is a normalization constant and

$$K_{\mathbf{0}_{||},\alpha,M}(t) = \frac{\sqrt{V_{\rm QW}}G_{\alpha,M}}{2\hbar}\int_{-\infty}^{t}E_{\mathbf{0}_{||},M}(s)\mathrm{e}^{\mathrm{i}\omega_{\mathbf{0}_{||},\alpha}s}\,\mathrm{d}s. \tag{14}$$

The important features of the exact solution (13) are the following.

(i) $|\Xi\rangle$ is a product of states of different excitonic modes, i.e. modes with different quantum numbers are not correlated. This is because the initial state was taken as the exciton vacuum, a product state, and because (12) is a sum over modes without inter-mode coupling.

(ii) Each factor in (13) is a Glauber coherent state. Therefore, under the approximations stated above, *the state of the QW interacting with a classical electromagnetic field is a multi-mode coherent state*. This is exactly the type of state which describes a coherent electromagnetic field such as that of a laser far above the threshold [27].

(iii) Each excitonic mode, $(\mathbf{0}_{||}, \alpha, M)$, is fully characterized by a single complex function $K_{\mathbf{0}_{||},\alpha,M}(t)$, which depends on the applied external field (see (14)).

Below, we show that these three features remain basically the same when we include disorder, breaking the translational invariance.

We now calculate the mean value of the exciton density and the induced electric dipole, which are quantities determined in the experiments. The expectation value of the occupation of the excitonic mode $(\mathbf{0}_{||}, \alpha, M)$ in the state (13) can be straightforwardly calculated. It is given by

$$\langle\Xi(t)|A^{\dagger}_{\mathbf{0}_{||},\alpha,M}A_{\mathbf{0}_{||},\alpha,M}|\Xi(t)\rangle = |K_{\mathbf{0}_{||},\alpha,M}(t)|^2 \tag{15}$$

while the total exciton density is $\sum_{\alpha,M}|K_{\mathbf{0}_{||},\alpha,M}(t)|^2$. With this, the $\mathbf{0}_{||}$ component of the laser-induced excitonic electric dipole density (the polarization) is

$$\langle\Xi(t)|\hat{\boldsymbol{P}}^{(+)}_{\mathbf{0}_{||}}|\Xi(t)\rangle = \sum_{\alpha,M}\frac{G_{\alpha,M}}{\sqrt{V_{\rm QW}}}\mathrm{i}\mathrm{e}^{\mathrm{i}\omega_{0,\alpha}t}K_{\mathbf{0}_{||},\alpha,M}(t)\vec{u}_M \tag{16}$$

which is linearly proportional to $E_{M,\mathbf{0}_{||}}(t)$. Due to the translational invariance along the QW plane, the expectation value of the other components vanishes. For an arbitrary propagation direction of the light, $\boldsymbol{k}_{L||}$, it can be shown that $\langle\hat{P}^{+}_{M,\boldsymbol{k}_{L||}}\rangle$ is the only nonzero component. The linear dependence of the induced electric dipole on the laser electric field is an *exact* property of both (1) and (12) as opposed to a result of the linear response approximation. If we performed such an approximation, we would obtain again the same result for the electric dipole, but *different* results for the exciton density or the quantum state of the system. It should be pointed out that (13) fulfills the coherence criteria of equation (11). A final point is the fact that the *total* induced dipole $\int P(r)\,\mathrm{d}V$ scales with $V_{\rm QW}$. It follows that the emitted intensity is superradiant [32] since it is proportional to $V^2_{\rm QW}$.

2.4. Exact solution including disorder

As we include the static disorder potential, we will find that most of the features of the disorder-free case remain the same. The main difference is that light with $\boldsymbol{k}_{||} = \mathbf{0}_{||}$ can now induce a nonzero expectation value of the dipole in *non-phase-matched* directions $\boldsymbol{k}_{||} \neq \mathbf{0}_{||}$.

In the case of the QW with disorder, the single-exciton eigenstates satisfy

$$\hat{h}_{\alpha}\ \psi_{\alpha,M,\xi}(\vec{\rho}) = e_{\alpha,\xi}\psi_{\alpha,M,\xi}(\vec{\rho}) \tag{17}$$

where $\hat{h}_{\alpha} \equiv (\frac{p^2}{2M_{\alpha}} + V_{\alpha}(\vec{\rho}))$ is the Hamiltonian for the centre of mass of the α-exciton interacting with the disorder potential $V_{\alpha}(\vec{\rho})$.

The operator that creates an exciton at $\vec{\rho}$ of type α and with third component of the angular momentum M can be obtained in both the plane-wave basis of the perfect crystal and the disorder basis:

$$\begin{aligned}\Psi^{\dagger}_{\alpha,M}(\vec{\rho}) &= \sum_{\boldsymbol{k}_{||}}\frac{\mathrm{e}^{\mathrm{i}\boldsymbol{k}_{||}\cdot\vec{\rho}}}{\sqrt{V_{\rm QW}}}A^{\dagger}_{\boldsymbol{k}_{||},\alpha,M}\\ &\equiv \sum_{\xi}\psi_{\alpha,M,\xi}(\vec{\rho})B^{\dagger}_{\xi,\alpha,M}.\end{aligned} \tag{18}$$

This leads to the following relationship between the old and the new operators:

$$A^{\dagger}_{\boldsymbol{k}_{||},\alpha,M} = \sum_{\xi}\frac{c_{\alpha,M,\xi}(\boldsymbol{k}_{||})}{\sqrt{V_{\rm QW}}}B^{\dagger}_{\xi,\alpha,M} \tag{19}$$

where

$$c_{\alpha,M,\xi}(\boldsymbol{k}_{||}) \equiv \int \mathrm{d}V\,\mathrm{e}^{\mathrm{i}\boldsymbol{k}_{||}\cdot\vec{\rho}}\psi_{\alpha,M,\xi}(\vec{\rho}) = \langle k_{||}|\alpha, M, \xi\rangle. \tag{20}$$

While, generally, an expression for these coefficients can only be obtained using numerical methods, we will later use an analytical approximation that gives good agreement with most experimental findings.

The excitonic part of the Hamiltonian, including disorder, can be written in terms of the new operators $B^{\dagger}_{\xi,\alpha,M}$ in the diagonal form

$$\hat{H}_{0D} = \hat{H}_0 + \hat{U} = \sum_{\xi,\alpha,M}\hbar\omega_{\xi,\alpha}B^{\dagger}_{\xi,\alpha,M}B_{\xi,\alpha,M} \tag{21}$$

where $\hbar\omega_{\xi,\alpha} = \hbar\omega_{\alpha} + \hbar\Delta_{\xi,\alpha}$, $\hbar\omega_{\alpha}$ is the centre of the lx or hx resonance and $\hbar\Delta_{\xi,\alpha} = e_{\alpha,\xi}$ is the distribution width. In a GaAs QW, the energies $\hbar\omega_{\alpha}$ are $\sim$1.5 eV and, in good samples, $\Delta_{\xi,\alpha}$ is distributed around zero with a width less than 1 meV.

The electric dipole operators can be written in terms of the new operators as

$$\hat{\boldsymbol{P}}^{(+)}_{\boldsymbol{q}_{||}} = \frac{1}{V_{\rm QW}}\sum_{\alpha,M,\xi}G_{\alpha,M}c_{\alpha,M,\xi}(\boldsymbol{q}_{||})B^{\dagger}_{\xi,\alpha,M}\vec{u}_M. \tag{22}$$

Inserting (22) in (10), we obtain

$$\hat{H}_{\rm int} = -\sum_{M,\alpha} G_{\alpha,M} E_{\mathbf{0}_{||},M} \sum_{\xi} (c_{\alpha,M,\xi}(\mathbf{0}_{||}) B^{\dagger}_{\xi,\alpha,M} + \text{c.c.}). \tag{23}$$

Notice that the classical electromagnetic field is again coupled linearly to the excitonic modes, so that the sum of (21) and (23) reduces again to a problem of driven harmonic oscillators. The main difference from the perfect crystal is that $E_{\mathbf{0}_{||},M}$ now couples to *all* the modes $B^{\dagger}_{\xi,\alpha,M}$.

Repeating the same steps as for the case without disorder, we obtain the exact collective wavefunction of the system and the expectation value of both the density and the induced electric dipole moment. Thus, assuming that for $t = -\infty$ all the modes are empty, the driven state at $t > -\infty$ is

$$|\tilde{\Xi}(t)\rangle = S \mathrm{e}^{\mathrm{i}H_{0D}t/\hbar} \prod_{\xi,\alpha,M} \exp(\mathrm{i}K^{\mathbf{0}_{||}}_{\xi,\alpha,M} B^{\dagger}_{\xi,\alpha,M})|0\rangle \tag{24}$$

where $S \equiv \prod_{\xi,\alpha,M} \exp(-|K^{\mathbf{0}_{||}}_{\xi,\alpha,M}|^2/2)$ and

$$\begin{aligned} K^{\mathbf{0}_{||}}_{\xi,\alpha,M}(t) &= \frac{G_{\alpha,M}\, c_{\xi,\alpha,M}(\mathbf{0}_{||})}{\hbar} \int_{-\infty}^{t} \mathrm{e}^{\mathrm{i}\omega_{\xi,\alpha}s} E_{\mathbf{0}_{||},M}(s)\, \mathrm{d}s \\ &= \frac{G_{\alpha,M}\, c_{\xi,\alpha,M}(\mathbf{0}_{||})}{\hbar} \tilde{E}(\omega_{\xi,\alpha}, t). \end{aligned} \tag{25}$$

As for the perfect crystal, this is a multi-mode Glauber coherent state with very similar properties to (13). All the considerations made for the case without disorder apply to (24). In particular, the excitonic modes that coupled to the laser field are coherent in the sense of equation (11).

We now calculate the expectation value of the exciton density and the induced electric dipole. The former is given by

$$\begin{aligned} &\langle\tilde{\Xi}(t)| \sum_{\xi,\alpha,M} B^{\dagger}_{\xi,\alpha,M} B_{\xi,\alpha,M} |\tilde{\Xi}(t)\rangle = \sum_{\xi,\alpha,M} |K^{\mathbf{0}_{||}}_{\xi,\alpha,M}(t)|^2 \\ &= \sum_{\xi,\alpha,M} \frac{G^2_{\alpha,M}}{\hbar^2} |c_{\xi,\alpha,M}(\mathbf{0}_{||})|^2 |\tilde{E}(\omega_{\xi\alpha}, t)|^2 \\ &= \sum_{\alpha,M} \frac{V_{\rm QW} G^2_{\alpha,M}}{4\pi^2\hbar^2} \int \mathrm{d}\omega_{\xi} \frac{\mathrm{d}\xi}{\mathrm{d}\omega_{\xi}} |c_{\omega_{\xi},\alpha,M}(\mathbf{0}_{||})|^2 |\tilde{E}(\omega_{\xi\alpha}, t)|^2 \end{aligned} \tag{26}$$

where $\frac{\mathrm{d}\xi}{\mathrm{d}\omega_{\xi}}$ is the density of states, whereas the $\boldsymbol{q}_{||}$ Fourier component of the induced electric dipole is

$$\begin{aligned} \langle \hat{\boldsymbol{P}}^{(+)}_{\boldsymbol{q}_{||}}(t)\rangle &= \sum_{\alpha M} \mathrm{e}^{-\mathrm{i}\omega_{\alpha}t} \Pi^{(+)}_{\alpha M \boldsymbol{q}_{||}} \vec{u}_M = \sum_{\alpha M} \mathrm{e}^{-\mathrm{i}\omega_{\alpha}t} \vec{u}_M \\ &\times \sum_{\xi} \frac{\mathrm{i}G_{\alpha,M}}{V_{\rm QW}} c^{*}_{\xi,\alpha,M}(\mathbf{0}_{||}) c_{\xi,\alpha,M}(\boldsymbol{q}_{||}) \tilde{E}(\omega_{\xi,\alpha}, t) \mathrm{e}^{\mathrm{i}\Delta_{\xi,\alpha}t} \end{aligned} \tag{27}$$

in agreement with the 'one-exciton' approach [25]. The *slowly varying* amplitude of the induced electric-dipole moment is denoted by $\Pi^{(+)}_{\alpha M \boldsymbol{q}_{||}}$. The most important feature of (27), compared to (16), is the fact that a laser with in-plane momentum $\boldsymbol{k}_{||} = \mathbf{0}_{||}$ induces dipoles in arbitrary directions $\boldsymbol{q}_{||} \neq \mathbf{0}_{||}$. This fact, due to the disorder potential, accounts for RRS observations in directions different from that of the laser [1, 3, 7, 9, 10].

Using (20), the closure relation for the basis defined by the solutions of (17) and

$$\mathrm{e}^{\mathrm{i}\hat{h}_{\alpha}t/\hbar}|\xi, \alpha, M\rangle = \exp(\mathrm{i}\mathrm{e}_{\alpha,\xi}t/\hbar)|\xi, \alpha, M\rangle, \tag{28}$$

we find that (27) can be written as

$$\langle \Pi^{(+)}_{\alpha,M,\boldsymbol{q}_{||}}(t)\rangle = \frac{G_{\alpha,M}}{V_{\rm QW}} \langle \boldsymbol{q}_{||}| \int_{-\infty}^{t} E_M(s) \mathrm{e}^{-\mathrm{i}\hat{h}_{\alpha}(s-t)/\hbar} |\boldsymbol{k}_{L||}\rangle. \tag{29}$$

In conclusion, the Glauber state picture of excitonic coherence in the linear regime [18] is also valid in the presence of a weak disorder potential. Disorder has two main consequences. First, each Fourier component of the laser field couples to *many* excitonic modes. Second, a laser field with well defined $\boldsymbol{k}_{||}$ induces electric dipoles with arbitrary Fourier component $\boldsymbol{q}_{||} \neq \boldsymbol{k}_{||}$.

2.5. Analytical ansatz for $c_{\xi,\alpha,M}(\boldsymbol{q}_{||})$

In the previous subsection, we derived exact general results concerning a gas of coherent excitons in a weak *arbitrary* disorder potential. Quantitatively, these results depend on the coefficients $c_{\xi,\alpha,M}(\boldsymbol{q}_{||})$, which can be obtained, in most cases, using numerical methods for diagonalizing the Hamiltonian. Another possibility is to perform averages over disorder configurations [25]. This is justified for experiments where the light emitted from different points of the sample is averaged over a wide angle [25]. After an average over configurations, disorder is described by a finite number of parameters (two in [25]). In order to obtain analytical expressions, we use a phenomenologically simpler, single-parameter ansatz, which agrees with many (although not all) experimental facts. It must be emphasized that the main qualitative results of our work are *independent* of the particular ansatz, which is only used to obtain analytically tractable results. More careful treatments of the problem of a single exciton in a weak disorder potential can be found in the literature [25, 33].

Any physically correct ansatz must obey the closure relation

$$\begin{aligned} &\sum_{\xi} \langle \boldsymbol{q}_{||}|\xi, \alpha, M\rangle\langle \xi, \alpha, M|\boldsymbol{q}_{||}\rangle = \sum_{\xi} |c_{\xi,\alpha,M}(\boldsymbol{q}_{||})|^2 \\ &= \frac{V_{\rm QW}}{4\pi^2} \int \frac{\mathrm{d}\xi}{\mathrm{d}\omega_{\xi}} \mathrm{d}\omega_{\xi} |c_{\omega_{\xi},\alpha,M}(\boldsymbol{q}_{||})|^2 = 1. \end{aligned} \tag{30}$$

Data from continuous-wave spectroscopy can be used to obtain information on $\frac{\mathrm{d}\xi}{\mathrm{d}\omega_{\xi}} |c_{\omega_{\xi},\alpha,M}(\mathbf{0}_{||})|^2$. In particular, optical absorption relates to the density of excitons created by a monochromatic laser of frequency Ω and helicity M. Considering (26), we have that

$$\begin{aligned} \mathcal{A}_M(\Omega) &\propto |E_0|^2 \sum_{\alpha} \frac{V_{\rm QW} G^2_{\alpha,M}}{4\pi^2\hbar^2} \\ &\times \int \mathrm{d}\omega_{\xi,\alpha} \frac{\mathrm{d}\xi}{\mathrm{d}\omega_{\xi,\alpha}} |c_{\omega_{\xi,\alpha},M}(\mathbf{0}_{||})|^2 \delta(\Omega - \omega_{\xi\alpha}). \end{aligned} \tag{31}$$

Experimentally, one finds that $\mathcal{A}_M(\Omega)$ can be approximated by a Lorentzian [8]. This suggests the ansatz

$$\frac{\mathrm{d}\xi}{\mathrm{d}\omega_{\xi}} |c_{\omega_{\xi,\alpha},M}(\boldsymbol{k}_{||})|^2 = \frac{4\pi\Gamma_{\alpha}}{V_{\rm QW}} \frac{1}{(\Delta_{\xi,\alpha})^2 + (\Gamma_{\alpha})^2} \tag{32}$$

where Γ_{α} is the disorder-induced broadening of the α exciton. If we put back (32) in (31) we obtain the Lorentzian form

$$\mathcal{A}_M(\Omega) \propto \sum_{\alpha} \frac{|E_0|^2\Gamma_{\alpha}}{\pi} \frac{1}{(\Omega - \omega_{\alpha})^2 + (\Gamma_{\alpha})^2} \tag{33}$$

where we took $|c_{\xi,\alpha,M}(\boldsymbol{k}_{||})|^2$ as an independent function of $\boldsymbol{k}_{||}$. Finally, we need to know $c^*_{\xi,\alpha,M}(\boldsymbol{0}_{||})c_{\xi,\alpha,M}(\boldsymbol{q})$ to compute (27). In the spirit of (32) we take

$$c^*_{\omega_\xi,\alpha,M}(\boldsymbol{0}_{||})c_{\omega_\xi,\alpha,M}(\boldsymbol{q}) = |c_{\omega_\xi,\alpha,M}|^2 \mathrm{e}^{-\mathrm{i}(\Phi_{q_{||}}(\omega_\xi)-\Phi_{k_{||}}(\omega_\xi))} \quad (34)$$

and

$$\delta \equiv \Phi_{\boldsymbol{q}_{||}}(\omega_\xi) - \Phi_{\boldsymbol{0}_{||}}(\omega_\xi) = \arctan\left(\frac{\Delta_{\xi,\alpha}}{\Gamma_\alpha}\right) \quad (35)$$

for the phase difference. As for $|c_{\xi,\alpha,M}(\boldsymbol{k}_{||})|^2$, we assume that the phase does not depend on $\boldsymbol{k}_{||}$ except for the trivial case $\boldsymbol{q}_{||} = \boldsymbol{0}_{||}$ and $\delta = 0$. Accordingly, within our ansatz, $\langle \hat{P}^{(+)}_{\boldsymbol{q}_{||},\alpha,M}(t)\rangle$ is the same for all $\boldsymbol{q}_{||} \neq \boldsymbol{0}_{||}$ but the phase-matched direction $\boldsymbol{0}_{||}$. Finally, we note that equation (35) is consistent with the orthogonality relation:

$$\sum_\xi \langle \boldsymbol{q}_{||}|\xi,\alpha,M\rangle\langle\xi,\alpha,M|\boldsymbol{k}_{||}\rangle = \delta_{\boldsymbol{k}_{||}\boldsymbol{q}_{||}}. \quad (36)$$

3. Coherent control of the exciton density

In this section, we give a microscopical description of the experiments on coherent control of the exciton density in GaAs QW reported in [2, 5, 6, 8]. In these experiments, samples at temperatures below 10 K were excited by a sequence of two identical *phase-locked* pulses. In Heberle *et al* [2] and Baumberg *et al* [6], the reflectivity change (ΔR), proportional to the density of photoexcited excitons [21], was measured as a function of τ. Marie *et al* [5] and Wörner and Shah [8] determined the exciton density from time-integrated luminescence data. In all these cases, the exciton density after excitation with two identical pulses can be fitted to the oscillatory form

$$\langle n_2\rangle = 2\langle n_1\rangle(1 + \mathcal{B}(\tau)\cos(\omega\tau)) \quad (37)$$

where $\langle n_1\rangle$ is the density created by a single pulse and ω is the exciton frequency. $\mathcal{B}(\tau)$, the amplitude of the oscillations, is smaller than unity and tends to zero for $\tau \gg T_2$.

3.1. Single mode

We begin our analysis with the case where a single heavy-hole exciton mode of frequency $\omega = E_{\mathrm{HH}}/\hbar$, $M = +1$ and coupling constant G is excited by the laser pulses [18]. This corresponds to the case of a perfect QW for which the hx–lx splitting is much bigger than the spectral width of the laser. We take the laser field as a circularly polarized plane wave, $E_M(t) = (F(t) + F(t-\tau))$, where

$$F(t) = E_0 \sin[\Omega t]\mathrm{e}^{-(\frac{t}{T})^2}. \quad (38)$$

T is the pulse duration, τ the delay and Ω the frequency of the spectral maximum of the laser. Following (15), the exciton density resulting from excitation by a single Gaussian pulse is [18]

$$\langle n_1(\omega)\rangle \approx \frac{G^2E_0^2T^2\pi}{4\hbar^2}\mathrm{e}^{-\frac{1}{2}[(\omega-\Omega)T]^2} \quad (39)$$

while the density due to two pulses for $t \gg T + \tau$ is

$$\langle n_2(\tau)\rangle = \left|\frac{G}{2\hbar}\int_{-\infty}^{+\infty} E(s)\mathrm{e}^{\mathrm{i}\omega s}\,\mathrm{d}s\right|^2$$
$$= \frac{G^2}{4\hbar^2}\tilde{F}(\omega)^2|(1+\mathrm{e}^{\mathrm{i}\omega\tau})|^2 = 2\langle n_1\rangle(1+\cos(\omega\tau)) \quad (40)$$

where $\tilde{F}(\omega)$ is the Fourier transform of the single-pulse electric field. It should be noted that, in order to obtain (40), it is a good approximation to replace the upper limit of integration in (14) by ∞.

Equation (40) ignores effects due to dephasing. Because of this, the two pulses continue to interfere for arbitrary long τ, i.e. $\mathcal{B}(\tau) = 1$ as opposed to $\mathcal{B}(\tau) \to 0$ for $\tau \to \infty$. The inelastic scattering contribution to dephasing is considered in section 7. Elastic scattering leading to coupling of light to a continuum of exciton modes is studied below.

3.2. Many modes

In a disordered QW, the laser excites a continuum of exciton modes. Using (26) and considering only the $M = +1$ hx-exciton, we obtain the multimode counterpart to (40)

$$n_2(\tau) = \sum_\xi |c_{\xi,\alpha,M}(\boldsymbol{0}_{||})|^2 2\langle n_1(\omega_\xi)\rangle(1+\cos(\omega_\xi\tau)) = \frac{V_{\mathrm{QW}}}{4\pi^2}$$
$$\times \int \frac{\mathrm{d}\xi}{\mathrm{d}\omega_\xi}\,\mathrm{d}\omega_\xi |c_{\xi,\alpha,M}(\boldsymbol{0}_{||})|^2 2\langle n_1(\omega_\xi)\rangle(1+\cos(\omega_\xi\tau)) \quad (41)$$

where $\langle n_1(\omega)\rangle$ is given by (39). This expression gives the photoexcited density as a sum over a distribution of modes. Since different modes have slightly different energies, their contributions cancel out as $\tau \to \infty$. We note that this result is independent of the particular form of the energy distribution function.

Now we use our ansatz (32) to compute (41) for the case where the central frequency of the laser pulse, Ω, is in resonance with the centre of the hx-distribution, ω_{H}. In this case, we have

$$\langle n_2\rangle = 2\langle n_1\rangle(1 + \mathcal{B}(\tau)\cos(\omega_{\mathrm{H}}\tau)). \quad (42)$$

The amplitude of the oscillations is

$$\mathcal{B}(\tau) = \mathrm{e}^{-\Gamma\tau}\mathrm{Erfc}\left[\frac{\Gamma T}{\sqrt{2}} - \frac{\sqrt{2}\tau}{2T}\right] + \mathrm{e}^{\Gamma\tau}\mathrm{Erfc}\left[\frac{\Gamma T}{\sqrt{2}} + \frac{\sqrt{2}\tau}{2T}\right] \quad (43)$$

where $\langle n_1\rangle$ is the density of excitons created by a single Gaussian pulse for a Lorentzian distribution of excitons. These results are plotted in figure 1. We see that, in contrast with the single-mode case, the amplitude $\mathcal{B}(\tau)$ decreases as τ increases, in agreement with the experimental findings [2,5,6,8]. The initial rise of $\mathcal{B}(\tau)$ observed in multi-QW samples [6] has been attributed to inter-well coupling, a problem that is not discussed in this paper. The decay of the coherence is discussed further in section 7.

4. Resonant Rayleigh scattering

Experimentally, a QW excited by a laser pulse with in-plane momentum $\boldsymbol{k}_{L||}$ emits light in all directions. Light

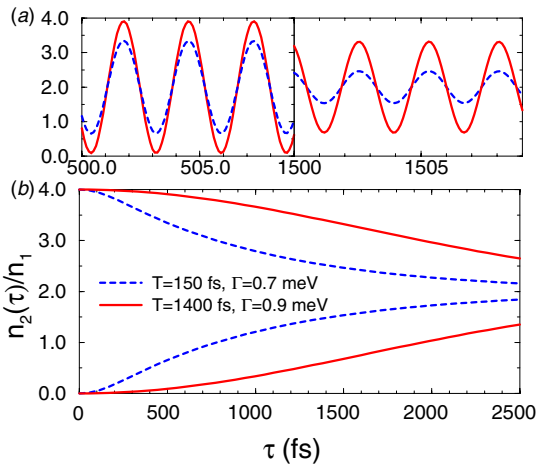

Figure 1. (*a*) Density of excitons created by two pulses, as a function of the delay τ. (*b*) Envelope function (following equation (43)) for two different values of Γ and T.

emitted in non-phase-matched directions ($\mathbf{q}_{||} \neq \boldsymbol{k}_{L||}$) is referred to as secondary emission. For secondary emission to occur, excitons must undergo in-plane momentum scattering. Examples include inelastic scattering with phonons and other excitons [34] and elastic scattering involving interface roughness and impurities. A remarkable experimental fact is that the secondary emission contains a coherent contribution [4, 7, 10, 11], in addition to incoherent photoluminescence [1]. Coherent secondary emission is also known as resonant Rayleigh scattering. This section is devoted to the understanding of RRS in the framework of our theory of coherent excitons as introduced in section 2. To this end, it is convenient to divide the main experimental observations into those that do not depend on the detection setup and those that do. Our model is intended to address the former case for which the primary findings are the following.

(i) The RRS intensity is linearly proportional to the intensity of the exciting laser [3, 7, 35].
(ii) RRS is coherent, i.e. it produces speckles [10] and its phase is correlated to that of the exciting laser [4, 7, 8, 11].
(iii) When both lx- and hx-excitons are created, the time dependence of the RRS intensity exhibits beatings of frequency $\omega_{\mathrm{L}} - \omega_{\mathrm{H}}$, the amplitude of which decays in $\sim$10 ps [1, 3, 7–9, 11, 12].
(iv) The RRS intensity has a finite rise time [1, 3, 7–9]. For short times and very low densities, the intensity is *quadratic* in time [3, 12].
(v) The RRS intensity decays for long times.

The understanding of geometry-dependent observations requires an analysis of the problem of a single exciton in a disorder potential that is more elaborate than our simple analytical ansatz. An example of detection-dependent observables is the behaviour of the scattering at long times for which [8, 9] and [3] report, respectively, an exponential and a power-law decay. We also note that, for a given sample, the single-speckle dynamics usually differs from the dynamics inferred from an average over the speckles [11], and that the results of single-speckle measurements depend on both the detection angle and the particular part of the sample that is excited [12, 36]. Moreover, samples with different disorder present differences in the single-speckle dynamics [10, 11]. Thus, RRS, i.e. light emitted by excitons that have not undergone any inelastic scattering process, is a tool to study the mesoscopic behaviour of excitons.

4.1. Quantum theory of RRS

In this part, we calculate using quantum mechanics the electromagnetic field emitted by the resonantly created excitons we studied in section 2. The primary reason we treat the non-phase-matched modes in quantum terms is that the expectation value of the occupation of these modes can be very low, so that a classical approximation cannot be justified *a priori*. As we will see, however, the secondary emission is coherent in the sense of Glauber so that a classical description applies as well [15].

From (1), the dynamics of the photon operator, $b_{k,M}$, is defined by the Heisenberg equation

$$\mathrm{i}\hbar \dot{b}_{\boldsymbol{k}_{||},k_z,\lambda}(t) = [b_{\boldsymbol{k}_{||}(t),k_z,\lambda}, H] = \hbar c|\boldsymbol{k}| b_{\boldsymbol{k}_{||},k_z,\lambda}(t) - \vec{\epsilon}_{\lambda,\boldsymbol{k}} \cdot \hat{\boldsymbol{P}}^{(-)}_{\boldsymbol{k}_{||}}(t) \sqrt{\left(\frac{\hbar c|k|}{2\epsilon_0 V}\right)} \tag{44}$$

the solution of which is given by

$$b_{\boldsymbol{k}_{||},k_z,\lambda}(t) = \mathrm{i}\hbar b_{\boldsymbol{k}_{||},k_z,\lambda}(t=0) - \sqrt{\left(\frac{\hbar c|k|}{2\epsilon_0 V}\right)} \int_0^t \mathrm{e}^{\mathrm{i}c|\boldsymbol{k}|(t'-t)} \vec{\epsilon}_{\lambda,\boldsymbol{k}} \cdot \hat{\boldsymbol{P}}^{(-)}_{\boldsymbol{k}_{||}}(t')\,\mathrm{d}t' \tag{45}$$

where $|\boldsymbol{k}| \equiv \sqrt{k_{||}^2 + k_z^2}$. The term $b_{\boldsymbol{k}_{||},k_z,\lambda}(t=0)$ reflecting fluctuations of the photon vacuum can be safely neglected in our case [27]. It is important to realize that, in the experiments, both the electric field amplitude and the scattered intensity are obtained by averaging over a large number of pulses. This average corresponds to the *quantum* expectation value of the electric field or the intensity operator. If we introduce (45) in the expression of the electric field (6) and calculate the average, we obtain

$$\langle \hat{\boldsymbol{E}}^{(+)}(\boldsymbol{r},t)\rangle \equiv \sum_{\boldsymbol{k}_{||},k_z,\lambda} \vec{\epsilon}_{\lambda,\boldsymbol{k}} \mathrm{e}^{\mathrm{i}\boldsymbol{k}\cdot\boldsymbol{r}} \left(\frac{\hbar c|k|}{2\epsilon_0 V}\right) \times \int_0^t \mathrm{e}^{\mathrm{i}c|\boldsymbol{k}|(t'-t)} (\vec{\epsilon}_{\lambda,\boldsymbol{k}} \cdot \langle \hat{\boldsymbol{P}}^{(-)}_{\boldsymbol{k}_{||}}(t')\rangle)\,\mathrm{d}t'. \tag{46}$$

This expression shows that whenever the induced electric dipole has a nonzero expectation value, so does the field associated with secondary emission, i.e. the secondary emission contains a coherent part. This is the case of a QW with disorder where a pulse with in-plane momentum $\boldsymbol{k}_{L||}$ creates an electric dipole whose Fourier components depend linearly on the electric field of the laser; see (27). Hence, our theory predicts that the emitted field in the presence of disorder has a well defined phase relation with the electric field of the laser pulse. This agrees with both the interferometry-based [4, 7, 8, 11] and the speckle [10] experiments. A more complete characterization of the photon state is given in appendix A, where we show that the photon state associated with RRS is a Glauber coherent state.

In most experiments, the parameter of interest is the intensity of the electromagnetic field [1, 3, 5, 9, 10]. Within

our formalism, and for a given polarization M, the intensity is given by [24, 27]

$$\langle I_M(t,\boldsymbol{r})\rangle = \langle E_M^{(-)}(\boldsymbol{r},t)E_M^{(+)}(\boldsymbol{r},t)\rangle \tag{47}$$

where $E_M^{(\pm)} \equiv \hat{\boldsymbol{E}}^{(\pm)}\cdot\vec{u}_M$. Combining the exact equations (27), (46) and (47), we find that the intensity of the secondary light emitted is proportional to the intensity of the exciting laser field, which agrees with the experiments.

Given M, the intensity of the coherent emission is [27]

$$\langle I_M^{\mathrm{coh}}(t,\boldsymbol{r})\rangle \equiv \langle \hat{E}_M^{(-)}(\boldsymbol{r},t)\rangle\langle \hat{E}_M^{(+)}(\boldsymbol{r},t)\rangle, \tag{48}$$

while the intensity of the incoherent part is $I_M^{\mathrm{inc}} \equiv \langle I_M(\boldsymbol{r},t)\rangle - \langle I_M^{\mathrm{coh}}(\boldsymbol{r},t)\rangle$. In appendix B, we show that (46) can be approximated by

$$\langle \hat{\boldsymbol{E}}^{(+)}(z,t)\rangle = \frac{\hbar\omega^2}{16\pi^2\epsilon_0 cz}\left\langle \hat{\boldsymbol{P}}^{(-)}\left(t-\frac{z}{c}\right)\right\rangle \tag{49}$$

in cases where the polarization is weakly dependent on $\boldsymbol{q}_{||}$. This applies to our ansätze (32) and (35). Therefore, the intensity of the coherent emission is

$$\langle I_M^{\mathrm{coh}}(\boldsymbol{r},t)\rangle \propto \langle \hat{P}_M^{(+)}(t)\rangle\langle \hat{P}_M^{(-)}(t)\rangle. \tag{50}$$

It is easy to see that the RRS intensity, $\langle I_M^{\mathrm{coh}}(\boldsymbol{r},t)\rangle$, is also linearly proportional to the intensity of the exciting laser.

4.2. Time dependence: finite rise time

We now calculate the early-time behaviour of the RRS. First, we show why the scattering has a finite rise time on the basis of the exact result (27) and assuming that the laser pulse can be represented by $\vec{E}(t) = E_0\vec{e}_\lambda\delta(t)$. In the calculations, we use the Gaussian pulse of (38); see appendix C. For a δ-pulse, (29) becomes

$$\langle \hat{\Pi}^{(+)}_{\boldsymbol{q}_{||},\alpha,M}(t)\rangle = E_0\frac{G_{\alpha,M}}{V_{\mathrm{QW}}}\langle \boldsymbol{q}_{||}|\mathrm{e}^{\mathrm{i}\hat{\hbar}_\alpha t/\hbar}|\boldsymbol{k}_{\boldsymbol{L}||}\rangle. \tag{51}$$

Recall that $\langle \hat{P}^{(+)}_{\boldsymbol{q}_{||},\alpha,M}(t=0)\rangle \propto \delta_{\boldsymbol{k}_{\boldsymbol{L}||},\boldsymbol{q}_{||}}$. This establishes a clear difference between the phase-matched ($\boldsymbol{k}_{\boldsymbol{L}||} = \boldsymbol{q}_{||}$) and non-phase-matched ($\boldsymbol{k}_{\boldsymbol{L}||} \neq \boldsymbol{q}_{||}$) directions since, initially, the phase-matched component of the induced electric dipole is the only one for which the expectation value does not vanish. The short-time behaviour of (51) can be derived from an expansion giving

$$\langle \hat{\Pi}^{(+)}_{\boldsymbol{q}_{||}}(t)\rangle \simeq \frac{E_0 G_{\alpha,M}}{V_{\mathrm{QW}}}((\mathrm{i}/\hbar)\langle \boldsymbol{q}_{||}|V_\alpha|\boldsymbol{k}_{\boldsymbol{L}||}\rangle)t \tag{52}$$

which shows that the amplitude of the induced dipole in arbitrary directions grows linearly with time. Combining (27), (50) and (52) we obtain the intensity at short times

$$I_M^{\mathrm{coh}} \propto t^2|\langle \boldsymbol{q}_{||}|V_\alpha|\boldsymbol{k}_{\boldsymbol{L}||}\rangle|^2 \tag{53}$$

(here, we omit the beating term, which also gives a quadratic rise). This result, a consequence of the unitary evolution of the excitons in the disorder potential, is in agreement with the RRS results of Haacke *et al* [3]. The quadratic rise has also been observed by other authors using different methods [17, 18, 23]. If the excitons undergo inelastic as well as elastic scattering, we expect the secondary emission to have an additional incoherent component, whose rise will not necessarily be quadratic. This is consistent with the experimental observation of a crossover to a linear rise at higher densities [3].

4.3. Time dependence: arbitrary times and lx–hx beats

We now show that $\langle I_M^{\mathrm{coh}}\rangle$ displays beats whenever both lx and hx are coherently excited. For simplicity, we assume that the exciting laser field has a well defined circular polarization, i.e. M is fixed. The intensity measured by a broadband detector can be written as

$$\begin{aligned}\langle I^{\mathrm{coh}}(\boldsymbol{r},t)\rangle \propto{}& \langle \Pi_{\mathrm{L}}^{(+)}(t)\rangle\langle \Pi_{\mathrm{L}}^{(-)}(t)\rangle + \langle \Pi_{\mathrm{H}}^{(+)}(t)\rangle\langle \Pi_{\mathrm{H}}^{(-)}(t)\rangle \\ &+2\cos[(\omega_{\mathrm{L}}-\omega_{\mathrm{H}})t]\mathrm{Re}\,[\langle \Pi_{\mathrm{L}}^{(+)}(t)\rangle\langle \Pi_{\mathrm{H}}^{(-)}(t)\rangle]\end{aligned} \tag{54}$$

where we have used equations (27) and (49). The first two terms reflect the intensity of the coherent RRS due to, respectively, lx and hx. The third term exhibits interferences that translate into beating between the lx- and hx-field. We note that our many-exciton approach differs significantly from the often-used picture of quantum beating of a three-level system [37]. The following arguments clarify this important point.

(i) The amplitude of the beats is nonzero as long as the mean electric dipole associated with *both* lx and hx and, by virtue of (46), the *amplitude* of the RRS field, is nonzero. In most papers where beats have been reported, the oscillations disappear in a time comparable to the inverse of the broadening (the decay time of the induced dipole). To the best of our knowledge, the only report of a direct measurement of both the intensity and the amplitude of the RRS is that by Wörner and Shah [8], who find that the amplitude of the field and that of the beats disappear nearly at the same time, in agreement with our model.

(ii) In general, there is no quantum entanglement between lx and hx. The exact solution of the problem, equation (24), is a *product* of lx- and hx-wavefunctions. Therefore, the state of the system cannot be described by an ensemble of excitons, each one in a linear superposition of lx- and hx-states. This statement does not apply to quantum dots or to the case considered in section 7 where a single exciton is present in the sample.

Up to this point, we have not made use of our analytical ansatz. To obtain an expression for RRS at arbitrary times, we insert our ansätze (32) and (35) in equation (27). For $\boldsymbol{q}_{||} \neq \boldsymbol{0}_{||}$, the induced dipole is independent of $\boldsymbol{q}_{||}$

$$\begin{aligned}\langle \hat{\boldsymbol{P}}^{(+)}(t)\rangle = {}& \sum_{\alpha,M}\vec{u}_M\mathrm{e}^{-\mathrm{i}\omega_\alpha t}4\pi G_{\alpha,M}\Gamma_\alpha \\ &\times\int_{-\infty}^{\infty}\frac{\mathrm{e}^{\mathrm{i}\arctan(\frac{\Delta_\alpha}{\Gamma_\alpha})}\mathrm{e}^{-\mathrm{i}\Delta_\alpha t}}{(\Delta_\alpha)^2+(\Gamma_\alpha)^2}\tilde{E}(\omega_\alpha+\Delta_\alpha,t)\,\mathrm{d}\Delta_\alpha\end{aligned} \tag{55}$$

where $\tilde{E}(\omega_\alpha+\Delta_\alpha,t)$ is defined in (25). When one probes individual speckles (small angular acceptance), RRS depends on both the emission direction and the region excited in the sample. As discussed earlier, our ansatz is not valid in such cases. On the other hand, our model can be applied to RRS measurements performed with large angular acceptance, which provide averaged information [25]. Using

$$\frac{1}{\pi}\int_{-\infty}^{\infty}\frac{\mathrm{e}^{\mathrm{i}\omega t}}{\omega^2+\Gamma^2}\mathrm{e}^{2\mathrm{i}\arctan(\frac{\omega}{\Gamma})}\,\mathrm{d}\omega = 2\Gamma t\mathrm{e}^{-\Gamma t} \tag{56}$$

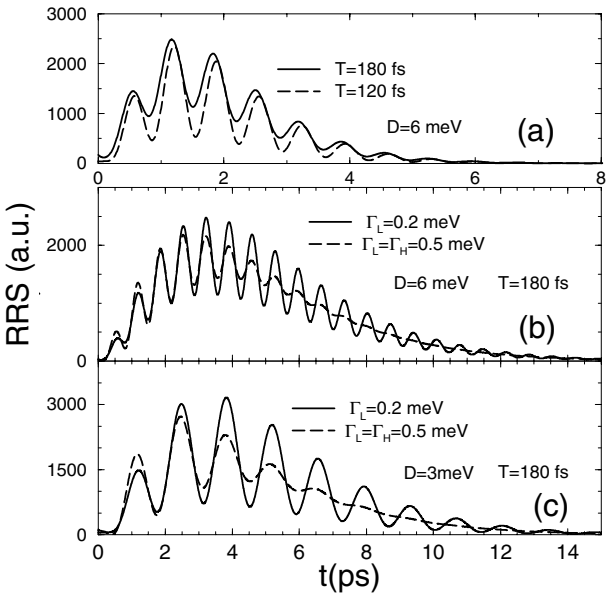

Figure 2. RRS as a function of time for different values of the pulse duration T, the excitonic broadenings $\Gamma_{\rm L}$ and $\Gamma_{\rm H}$ and the lx–hx splittings. Note that (*a*) has a different timescale and $\Gamma_{\rm L} = \Gamma_{\rm H} = 0.5$ meV.

and (25), we have

$$\langle \hat{\boldsymbol{P}}^{(+)}(t)\rangle = \sum_{\alpha,M} \frac{{\rm i}G_{\alpha,M}\Gamma_\alpha}{4\pi^2}\vec{u}_M \times \int_{-\infty}^{t} (t-s){\rm e}^{-(\Gamma_\alpha - {\rm i}\omega_\alpha)(t-s)}E(s)\,{\rm d}s. \tag{57}$$

For δ-pulses $E(t) = \sum_M E_0\delta(t)\vec{u}_M$ we trivially obtain

$$\langle \hat{\boldsymbol{P}}^{(+)}(t)\rangle = E_0 \sum_{\alpha,M} \frac{{\rm i}G_{\alpha,M}\Gamma_\alpha}{4\pi^2} 2t{\rm e}^{-(\Gamma_\alpha - {\rm i}\omega_\alpha)t}\vec{u}_M. \tag{58}$$

It is apparent that, in this expression, Γ_α plays the role of the decay rate. For short times, the induced dipole in the non-phase-matched direction grows linearly with t, leading to a quadratic rise in the RRS intensity. The maximum of the intensity (for either lx or hx) is $T_{\alpha R} = 1/\Gamma_\alpha$, which is twice the decay time.

Results for Gaussian pulses are shown in figure 2. In all cases, the laser is spectrally peaked 6 meV below the hx-resonance. In figure 2(*a*), the RRS intensity is shown for two values of the laser pulse-width, T. Note that the amplitude of the beats diminishes with increasing width as the population of lx becomes smaller. As shown by the comparison between figures 2(*a*) and (*b*), the effect of increasing the decay of the lx-exciton is to accelerate both the rise and the decay of the beat amplitude. Finally, figure 2(*c*) uses the same parameters as in figure 2(*b*) except for the lx–hx splitting D, which, being smaller, gives a larger beating period.

It should be noted that the expectation value of $A_{q_{||},\alpha,M}$, evaluated with the state (24) and using the ansätze (32) and (35), decays as a function of time. This is in contrast with the behaviour of the expectation value of the operators $B_{\xi,\alpha,M}$ which oscillate but do not decay. As discussed in section 7, the decay of the plane-wave operators can be understood as the result of destructive interference between coherent disorder modes. The decay of the total electric dipole has also been obtained in the so-called classical model, where the exciton is treated as a particle with infinite mass [17]. We conclude this section by emphasizing that, other than for (55), (57) and (58), our results are independent of the model used to describe the disorder.

5. Coherent control of the exciton spin

This section focuses on the GaAs QW measurements of Marie *et al* [5] involving coherent control of the exciton spin. Their setup relies on two mode-locked 1.4 ps laser pulses that are oppositely polarized, delayed by τ, and both resonant with the hx-state. What is measured is the polarization state of the secondary emission. The experiments use two configurations. In one case, they excite with circularly polarized $(+,-)$ pulses and detect the degree of linear polarization of the secondary radiation

$$\mathcal{P}_l(t,\tau) = \frac{I_x(t,\tau) - I_y(t,\tau)}{I_x(t,\tau) + I_y(t,\tau)} \tag{59}$$

whereas, in the other, they excite with linearly polarized (x, y) pulses and probe the degree of circular polarization

$$\mathcal{P}_c(t,\tau) = \frac{I_{+1}(t,\tau) - I_{-1}(t,\tau)}{I_{+1}(t,\tau) + I_{-1}(t,\tau)}. \tag{60}$$

In either case, Marie *et al* [5] find that the relevant parameter is an oscillating function of $\omega_{\rm H}\tau$. Moreover, the amplitude of the oscillations decays exponentially, *as a function of* τ, in $\sim$6 ps. This time is of the order of typical decay times of the induced electric dipole. These results raise the question as to whether or not the secondary emission can be ascribed to (coherent) RRS. In what follows, we prove that the fact that $\mathcal{P}_l$ and $\mathcal{P}_c$ can be coherently controlled necessarily implies that the secondary emission contains a coherent component. Thus, the work of Marie *et al* can be added to the list of experiments that reveal partial coherence of the secondary emission as in recent interferometric work [4, 7, 8, 11] and the analysis of speckle statistics [10]. Another important experimental finding of Marie *et al* is that, for a fixed value of τ, both $\mathcal{P}_l$ and $\mathcal{P}_c$ decay *as a function of the detection time* at, respectively, rates $T_{s1} \neq T_{s2}$, which are also different from T_2. This means that exciton coherence and spin coherence are different phenomena [38] and also that the relaxation mechanisms [39] are independent of the way in which spin polarizations are created (e.g. with one or two pulses). As shown below, our theory of coherent excitons in a weak disorder potential explains these experimental facts.

5.1. Circular excitation, linear detection

In this subsection we consider in detail the experiment in which the QW is excited by two circularly polarized pulses and the linearly polarized component of the secondary emission, $\langle I^X(t)\rangle$ and $\langle I^Y(t)\rangle$, are recorded. Our main result below is that the linear polarization of the coherent part is the only component that can be coherently controlled. The case of linear excitation and circular detection is practically identical; the corresponding results are summarized in the next section.

Using (47), and splitting the electric field into coherent ($\langle E\rangle$) and incoherent (δE) components we write

$$\langle I_{X,Y}(t)\rangle \equiv \langle E^{(-)}_{X,Y}(t)\rangle\langle E^{(+)}_{X,Y}(t)\rangle + \langle \delta E^{(-)}_{X,Y}(t)\delta E^{(+)}_{X,Y}(t)\rangle = \langle I^{\rm coh}_{X,Y}\rangle + \langle I^{\rm incoh}_{X,Y}\rangle. \quad (61)$$

Focusing on the incoherent part, we use (49) to write

$$\langle I^{\rm incoh}_{X,Y}\rangle = \tfrac{1}{2}\sum_{M=\pm1}\langle \delta P^{(+)}_M \delta P^{(-)}_M\rangle \pm \tfrac{1}{2}(\langle \delta P^{(+)}_{+1}\delta P^{(-)}_{-1}\rangle + \text{c.c.}) \quad (62)$$

where we have used

$$\vec{u}_x = \frac{1}{\sqrt{2}}(\vec{u}_{+1}+\vec{u}_{-1}) \qquad \vec{u}_y = \frac{1}{\mathrm{i}\sqrt{2}}(\vec{u}_{+1}-\vec{u}_{-1}).$$

Now we show that only the diagonal part of $\langle I^{\rm incoh}_{X,Y}\rangle$, that is, the first term in (62), is nonzero. The second term measures the correlation between spin-up and spin-down excitons, which vanishes in the noninteracting picture. At the low densities at which the experiments are performed, we expect the corresponding term in the coherent part, namely, $\langle P^{(+)}_{+1}\rangle\langle P^{(-)}_{-1}\rangle$, to dominate over the correlation term, even in the case where the excitons interact. Thus, we have

$$\langle I^{\rm incoh}_X\rangle - \langle I^{\rm incoh}_Y\rangle = 0 \quad (63)$$

so the incoherent part of the emission cannot be coherently controlled. We now turn our attention to the coherent component of the radiation. In equation (50), we introduce the expectation value of the induced electric dipole in non-phase-matched directions

$$\langle P^{(+)}(t,\tau)\rangle = \mathrm{e}^{-\mathrm{i}\omega_{\rm H}t}\Pi^{(+)}_{+1}(t)\vec{u}_{+1} + \mathrm{e}^{-\mathrm{i}\omega_{\rm H}(t-\tau)}\Pi^{(+)}_{-1}(t-\tau)\vec{u}_{-1} \quad (64)$$

and obtain

$$\langle I^{\rm coh}_{X,Y}(t)\rangle = \tfrac{1}{2}\Pi^{(+)}_{+1}(t)\Pi^{(-)}_{+1}(t) + \tfrac{1}{2}\Pi^{(+)}_{-1}(t-\tau)\Pi^{(-)}_{-1}(t-\tau) \pm \mathrm{Re}\,[\mathrm{e}^{\mathrm{i}\omega_{\rm H}\tau}\Pi^{(+)}_{+1}(t)\Pi^{(-)}_{-1}(t-\tau)]. \quad (65)$$

Thus, we have

$$\mathcal{P}_l(t,\tau) = \frac{2\mathrm{Re}\,[\mathrm{e}^{\mathrm{i}\omega_{\rm H}\tau}\Pi^{(+)}_{+1}(t)\Pi^{(-)}_{-1}(t-\tau)]}{\Pi^{(+)}_{+1}(t)\Pi^{(-)}_{+1}(t)+\Pi^{(+)}_{-1}(t-\tau)\Pi^{(-)}_{-1}(t-\tau)}. \quad (66)$$

In agreement with the experiments, and independently of the form of $\Pi^{(+)}_M(t)$, the numerator of this expression is proportional to $\cos(\omega_{\rm H}\tau)$. We see that, for the interference to take place, we need the electric dipoles induced both by the first pulse $\Pi^{(+)}_{+1}(t)$ and by the second pulse $\Pi^{(-)}_{-1}(t-\tau)$ to be nonzero at the same time.

To provide a quantitative comparison, we use our ansatz to obtain an analytical approximation for $\mathcal{P}_l(t)$. For simplicity, we assume δ-pulses, which can be safely done because only hx-excitons are involved. With these approximations we obtain $\Pi^{(+)}_{+1}(t) = \mathrm{i}\Gamma_{\rm H}G_{\rm H}t\mathrm{e}^{-\Gamma t}$ and $\Pi^{(+)}_{-1}(t-\tau) = \mathrm{i}\Gamma_{\rm H}G_{\rm H}\theta(t-\tau)(t-\tau)\mathrm{e}^{-\Gamma(t-\tau)}\mathrm{e}^{\mathrm{i}\omega_{\rm H}\tau}$. Replacing the latter expressions in (66), we obtain the RRS intensity along the x- and y-axes determined in the experiments. The analytical expression for the degree of linear polarization is given by

$$\mathcal{P}_l(t,\tau) = \frac{2t(t-\tau)\mathrm{e}^{\Gamma\tau}\theta(t-\tau)\cos(\omega_{\rm H}\tau)}{t^2+\mathrm{e}^{2\Gamma\tau}\theta(t-\tau)(t-\tau)^2}. \quad (67)$$

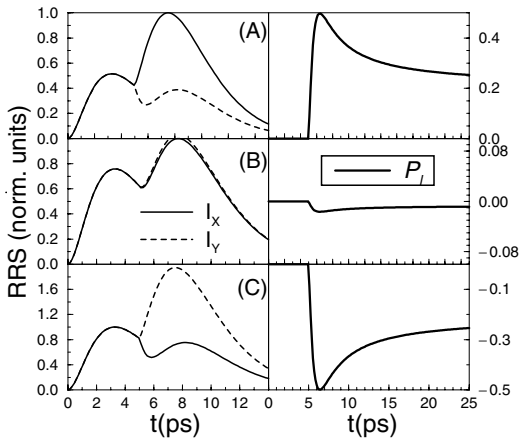

Figure 3. Left panels: RRS linear components (x and y) after excitation with $M = +1$ at $t = 0$ fs and $M = -1$ at (a) 5002.5 fs, (b) 5003.25 fs and (c) 5003.95 fs, with $\Gamma_h = 0.3$ meV. RRS intensity is normalized in units of the maximum of I_X. Right panels: P_l (see equation (67)).

Results are displayed in figures 3(a)–(c). In all the calculations, a circularly polarized laser pulse ($M = +1$) excites the QW at $t = 0$ and a second counter-polarized pulse ($M = -1$) excites the QW at various delay times. Before the second pulse arrives at the sample, we have $I_x - I_y = 0$. When the second pulse arrives, $I_x - I_y$ becomes positive (a), zero (b), or negative (c) depending on the value of τ. In the right-hand panels of figure 3, we show the behaviour of $\mathcal{P}_l$ as a function of t for a fixed value of τ. $\mathcal{P}_l = 0$ before the second pulse arrives. The absolute value of $\mathcal{P}_l$ increases when the second pulse arrives, tending towards $\mathrm{e}^{-\Gamma\tau}\cos(\omega_{\rm H}\tau)$, for $t \gg \tau$. This means that, within our model, the linear degree of polarization does not decay to zero as a function of the detection time, i.e. the spin coherence time ($T_{2\rm s}$) is different from the optical coherence time T_2. Accordingly, additional spin relaxation mechanisms need to be included in the model to match the experimental observations.

Coherent control of the linear polarization is illustrated in figure 4. The oscillations of $\mathcal{P}_l$ as a function of $\omega_{\rm H}\tau$ are shown for $t = 4$ ps $+ \tau$, as in the experiments [5]. The figure also shows the calculated amplitude of the oscillations for two values of the hx broadening parameter. Our results are in good qualitative agreement with the experimental data.

5.2. Linear excitation, circular detection

The discussion of the previous subsection can be easily modified so that it applies to the case of linear excitation and circular detection. The main results are the following.

(i) Only the circularly polarized component of the coherent emission can be coherently controlled. $\mathcal{P}_c(t,\tau)$ is given by

$$\frac{2\mathrm{Re}\,[\mathrm{i}\mathrm{e}^{\mathrm{i}\omega_{\rm H}\tau}\Pi^{(+)}_x(t)\Pi^{(-)}_y(t-\tau)]}{\Pi^{(+)}_x(t)\Pi^{(-)}_x(t)+\Pi^{(+)}_y(t-\tau)\Pi^{(-)}_y(t-\tau)}. \quad (68)$$

Coherent control results when the linear dipoles induced by the two pulses do not vanish at the same time.

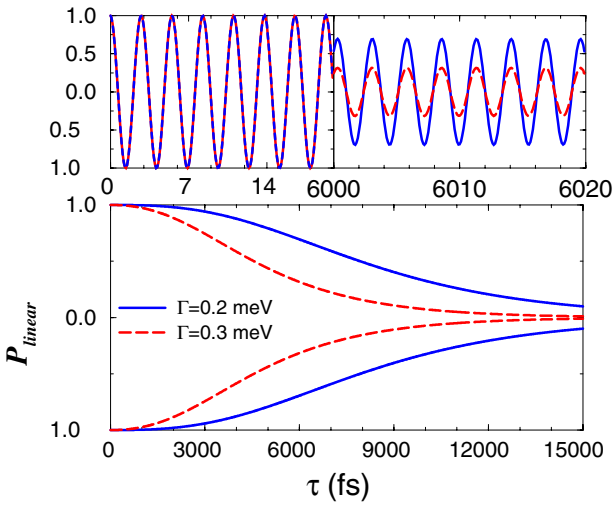

Figure 4. Coherent control of the linear polarization. In the upper part of the figure we plot P_l as a function of τ. In the lower part of the figure we plot the amplitude of the coherent control oscillations as a function of τ for two different values of the parameter Γ. The detection time is $t = \tau + 4$ ps in both parts of the figure.

(ii) The expression for the circular polarization of the RRS calculated with our ansatz (35) is

$$\mathcal{P}_c(t,\tau) = \frac{2t(t-\tau)e^{\Gamma\tau}\theta(t-\tau)\sin(\omega_H\tau)}{t^2 + e^{2\Gamma\tau}\theta(t-\tau)(t-\tau)^2}. \quad (69)$$

(iii) For a fixed value of τ and long detection time $\mathcal{P}_c(t,\tau) = e^{-\Gamma\tau}\sin(\omega_H\tau)$. That is, in our model the linear degree of polarization does not decay to zero as a function of the detection time. Because of this, a mechanism of longitudinal spin relaxation would need to be included to account for the experimentally observed decay T_{s1}.

6. Coherent control of resonant Rayleigh scattering

In this section, we consider the experiments of Garro *et al* [9] on coherent control of RRS using two identically polarized pulses to attain control of the hx–lx beat amplitude. A very similar experimental configuration was used by Wörner and Shah [7] in their measurements of the RRS field amplitude.

In Garro *et al* [9], the first pulse creates a coherent population of both hx- and lx-excitons (note that this is in contrast with [5] where only hx-excitons are generated). When the second pulse strikes, the subsequent RRS beating amplitude is enhanced (suppressed) if the time-delay between the two pulses coincides with a maximum (minimum) of the RRS beats due to the first pulse.

To understand this effect, consider the induced electric dipole, which is the sum of four terms (the light is circularly polarized) corresponding to the hx- and lx-polarizations created by the first and the second pulse:

$$\langle P(t)\rangle = \langle P^{(+)}_{1L}(t) + P^{(+)}_{1H}(t) + P^{(+)}_{2L}(t-\tau) + P^{(+)}_{2H}(t-\tau)\rangle. \quad (70)$$

Therefore, the RRS intensity has 16 components which can be classified into nine sets. First, we have the terms $I_{11L} = \langle\Pi^{(+)}_{1L}(t)\rangle\langle\Pi^{(-)}_{1L}(t)\rangle$, $I_{11H} = \langle\Pi^{(+)}_{1H}(t)\rangle\langle\Pi^{(+)}_{1H}(t)\rangle$ and

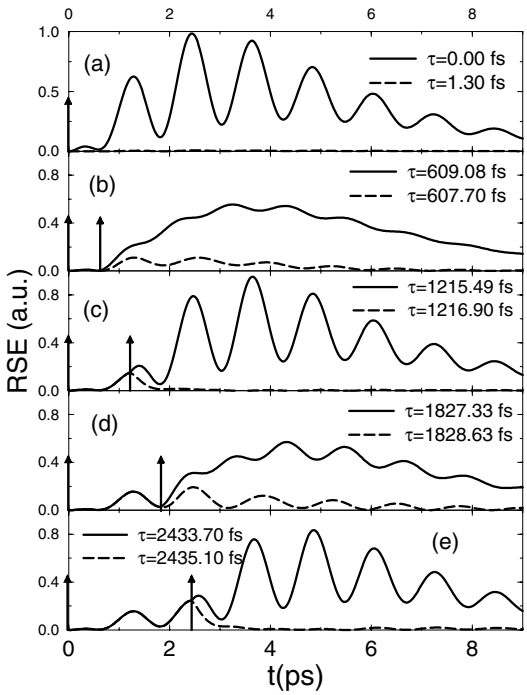

Figure 5. RRS for a QW excited with two pulses, the first at $t = 0$ and the second at $t = \tau$ with (*a*) $\tau \simeq 0$, (*b*) $\tau \simeq 0.6$ ps, (*c*) $\tau \simeq 1.2$ ps, (*d*) $\tau \simeq 1.8$ ps and (*e*) $\tau \simeq 2.4$ ps. Solid (dashed) curves = constructive (destructive) interference. $\Gamma_h = 0.20$ meV, $\Gamma_l = 0.34$ meV.

$I_{11HL} = \langle\Pi^{(+)}_{1L}(t)\rangle\langle\Pi^{(-)}_{1H}(t)\rangle + \text{c.c.}$, which correspond to RRS due to the first pulse (lx-, hx-emission and beating). The corresponding terms for the second pulse are I_{22L}, I_{22H} and I_{22HL}. The standard coherent control of the lx-density is associated with $I_{CCL} = \langle\Pi^{(+)}_{1L}(t)\rangle\langle\Pi^{(-)}_{2L}(t-\tau)\rangle e^{i\omega_L\tau} + \text{c.c.}$, with a similar expression for I_{CCH}. Finally, $I_{CCbeat} = \langle\Pi^{(+)}_{1L}(t)\rangle\langle\Pi^{(-)}_{2H}(t-\tau)\rangle e^{-i(\omega_L-\omega_H)t+i\omega_H\tau} + \langle\Pi^{(+)}_{1H}(t)\rangle\langle\Pi^{(-)}_{2L}(t-\tau)\rangle e^{i(\omega_L-\omega_H)t+i\omega_L\tau} + \text{c.c.}$ reflects RRS-beat interference due to both pulses. Results using our analytical ansatz are shown in figures 5(*a*)–(*e*) for various values of τ. In the figure, the solid (dashed) curves correspond to delays that produce constructive (destructive) interference. In figure 5(*a*) the delay between pulses is almost zero, so the patterns of constructive and destructive control are enhanced. In figures 5(*c*) and (*e*) the second pulse arrives when the RRS-beating due to the first pulse is largest, so beating is *enhanced*. The opposite situation, i.e. beating suppression, is illustrated in figures 5(*b*) and (*d*). The calculations are in excellent agreement with experiments.

Figure 6 (top) shows one of most interesting features of coherent control in that dramatic changes in the RRS intensity can be achieved by extremely small (∼1 fs) changes in the delay τ. This effect stems from the coherent control terms, $I_{CCH} + I_{CCL}$. The top and bottom panels of figure 6 correspond, respectively, to RRS-beating enhancement and suppression. The insets show the RRS contribution due to hx ($I_{11H} + I_{22H} + I_{12H}$) and lx alone ($I_{11L} + I_{22L} + I_{12L}$). In the case of amplitude enhancement, we see that the lx- and hx-populations increase when the second pulse arrives with the proper phase for constructive interference. The reverse case is represented in the bottom panel. This can be understood

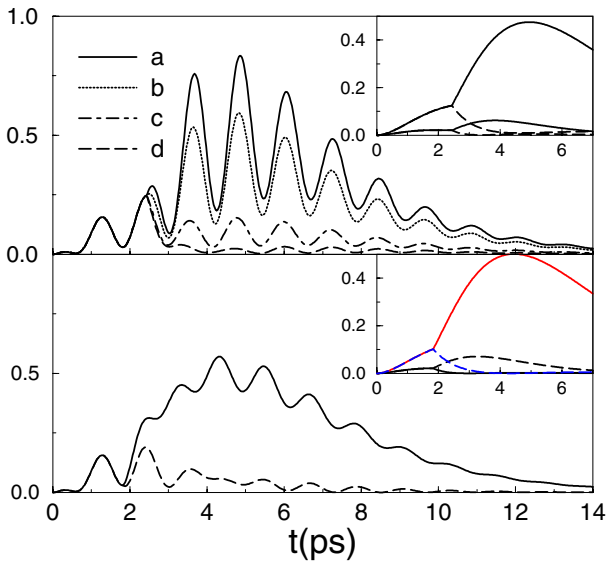

Figure 6. RRS in the case of enhancement (upper part) and suppression (lower part). Upper part (a) $\tau = 2433.7$ fs, (b) $\tau = 2434.25$ fs, (c) $\tau = 2434.75$ fs, and (*d*) $\tau = 2435.0$ fs. Inset: total hx- and lx-emission for (a)–(c). Lower part. Solid curve $\tau = 1827.3$ fs and dashed curve $\tau = 1828.1$ fs. In all cases we fix $\Gamma_h = 0.20$ meV, $\Gamma_l = 0.34$ meV and the lx–hx splitting is 3.4 meV.

as follows. In the case of enhancement, we have $\delta\tau \equiv (\omega_L - \omega_H)\tau = 2N\pi$, where N is an integer. When the second pulse enhances the hx-population $\omega_H\tau = 2N'\pi$, where N' is also an integer. We can then write $\omega_L\tau = (\delta + \omega_H)\tau = 2\pi(N + N')$, so the lx-population is also larger. In the case of destructive interference, we have $\delta\tau = (2N + 1)\pi$. Thus, when the second pulse leads to a larger hx-population we have $\omega_H\tau = 2N'\pi$. Hence, $\omega_L\tau = (\delta + \omega_H)\tau = \pi + 2\pi(N + N')$, so the lx-population becomes smaller when the population of hx-excitons becomes larger, and vice versa. The case of global constructive interference (solid curve) corresponds to hx-enhancement with the consequent lx-suppression. This configuration is interesting given that selective excitation of lx and hx is not possible with single-pulse excitation.

7. Discussion

In the previous sections, we applied our microscopic theory to the analysis of various interference phenomena. Here, we address the questions of the origin of the coherence decay (*elastic* versus *inelastic*) and the oscillatory behaviour (*quantum* versus *classical*).

7.1. Dephasing

In the linear experiments, the amplitude of the interference decays at long times (and at long τ in the two-pulse experiments). Generally speaking, the decay reflects two independent mechanisms [40]:

(1) destructive interference of an ensemble of coherent modes with slightly different energies (inhomogeneous broadening) and
(2) inelastic scattering (or homogeneous broadening) leading to $\langle B_\xi^+ + B_\xi \rangle = 0$ for $t \to \infty$.

The first one, specifically, disorder-induced elastic scattering, is the decay mechanism considered in this paper. Following the impulsive excitation, the eigenmodes are initially in phase but, as some modes evolve faster than others, they interfere destructively, so the total electric dipole goes to zero in a time of the order of the inverse of the broadening. This decay occurs even if the individual modes remain coherent in the sense that $\langle B_{\xi,\alpha,M} \rangle \neq 0$.

Inelastic processes were not included in our calculations, although we could have done so phenomenologically by simply adding a small imaginary component to the exciton energy or using the density matrix formalism to take into account the interactions between excitons and other excitations such as phonons and unbound electron–hole pairs. Within the context of our results, we notice the well known approach to calculate the density matrix using coherent states as the basis [15, 27].

In general, both elastic and inelastic processes contribute to the dephasing. For the experiments considered in this paper, the inhomogeneous broadening is $\gtrsim$0.1 meV, in most cases. This should be compared with values for the homogeneous component, inferred from four-wave-mixing (FWM) [41] and near-field methods [42], which are typically 0.01–0.1 meV at low temperatures. Therefore, the decay of the macroscopic electric dipole, at low temperatures, is mainly due to the inhomogeneous broadening. In this situation, light emission from the QW differs from that of an incoherent population of excitons in that it shows a speckle pattern [10] as opposed to incoherent luminescence [28].

7.2. Macroscopic versus microscopic coherent control

What is the physical origin of the coherent control discussed in section 3? Here, we show that there are generally two very different alternatives, which we refer to as *macroscopic* and *microscopic*, and that all the phenomena considered in this paper belong to the first type. Consider the state of the exciton field after excitation by two pulses. Assuming that only hx-excitons with $M = +1$ are created, we have

$$|\tilde{\Xi}(t)\rangle = S e^{iH_{0D}t/\hbar} \prod_\xi \exp[i(K_{\xi 1}^{\mathbf{0}_\parallel} + K_{\xi 2}^{\mathbf{0}_\parallel}) B_{\xi,\alpha,M}^\dagger]|0\rangle \quad (71)$$

where $K_{\xi 1}^{\mathbf{0}_\parallel}$ and $K_{\xi 2}^{\mathbf{0}_\parallel}$, as defined in (25), correspond to the first and second pulse. It is apparent that this wavefunction *is not a sum* of the states that result from the independent excitation of the pulses. This should be contrasted with the expression for the electric dipole

$$\langle P^{(+)}(t) \rangle = \langle P_1^{(+)}(t) \rangle + \langle P_2^{(+)}(t) \rangle \quad (72)$$

which, due to the linearity of the problem, *is a sum* of the dipoles created by each pulse. Therefore, the interference stems from the fact that the energy absorbed by the QW is proportional to $\langle P^{(+)}(t) \rangle \langle P^{(-)}(t) \rangle$, which contains the cross term $\langle P_1^{(+)}(t) \rangle \langle P_2^{(-)}(t) \rangle$ + c.c.. This we label *macroscopic* coherent control because the interference is associated with the macroscopic electric dipole. Similar arguments apply to coherent control experiments involving phonons [43] and polaritons in microcavities [44].

We consider now the limit of very low excitation so that only one exciton is present in the sample. This situation is similar to the problem of a single atom [45] or a quantum dot [46]. In this case, we can truncate (71) to obtain

$$|\tilde{\Xi}(t)\rangle = S\mathrm{e}^{\mathrm{i}H_{0D}t/\hbar}\left(1+\sum_{\xi}\mathrm{i}[K_{\xi 1}^{\mathbf{0}_{||}}+K_{\xi 2}^{\mathbf{0}_{||}}]B_{\xi,\alpha,M}^{\dagger}\right)|0\rangle. \quad (73)$$

This state represents an exciton in a quantum superposition of two alternatives: the exciton is created either by the first or by the second pulse. This is what we call *microscopic* coherent control. Measurements that probe the excited state population will generally show an oscillatory behaviour (the so-called Ramsey oscillations [47]) as a function of the delay time.

7.3. Classical versus quantum beats

We now return to the question of the classical versus quantum nature of the lx–hx beats. The arguments follow closely those of the previous subsection. Following impulsive excitation, the state of the system is

$$S\mathrm{e}^{\mathrm{i}H_{0D}t/\hbar}\prod_{\xi}\exp[\mathrm{i}(K_{\xi\mathrm{L}}^{\mathbf{0}_{||}})B_{\xi,\mathrm{L}}^{\dagger}]\exp[\mathrm{i}(K_{\xi\mathrm{H}}^{\mathbf{0}_{||}})B_{\xi,\mathrm{H}}^{\dagger}]|0\rangle$$
$$= S\mathrm{e}^{\mathrm{i}H_{0D}t/\hbar}\exp\left(\sum_{\xi,\alpha}\mathrm{i}(K_{\xi\alpha}^{\mathbf{0}_{||}})B_{\xi,\alpha}^{\dagger}\right) \quad (74)$$

where we have omitted the quantum number M. This expression tells us that the state of the system is *not* a sum state of lx plus hx (or a product of sum states), but the exponential of a sum. As we have seen in section 2, (74) carries an electric dipole which can be written as the *sum* of two oscillating dipoles of frequencies ω_{L} and ω_{H}. It is clear that, as long as the dipole amplitudes are nonzero, the intensity of the light emitted by our system will exhibit beats as a function of time. Thus, unlike atomic systems [48], lx–hx beating is not the result of quantum interference. Here, it may be argued that there is no fundamental distinction between (74) and the leading term in the expansion in powers of the field

$$S\mathrm{e}^{\mathrm{i}H_{0D}t/\hbar}\left[1+\sum_{\xi}\mathrm{i}(K_{\xi\mathrm{L}}^{\mathbf{0}_{||}})B_{\xi,\mathrm{L}}^{\dagger}+\mathrm{i}(K_{\xi\mathrm{H}}^{\mathbf{0}_{||}})B_{\xi,\mathrm{H}}^{\dagger}\right]|0\rangle \quad (75)$$

which *is* a quantum superposition state of lx- and hx-excitons. The problem with this is that the leading term represents a state with only one exciton in the illuminated volume of the QW while the exact state (74) describes one with a number of excitons of order $\sum|K_{\xi\alpha}^{\mathbf{0}_{||}}|^2 \sim V_{\mathrm{QW}}$. Hence, it is only in the limit where there is one (or a few) excitons in the sample that the Glauber state can be approximated by a quantum-entangled state for which the beats become conceptually similar to those of atom-like systems such as quantum dots and localized exciton states [46]. It is important to notice that the transition from the many-exciton Glauber state to the quantum-beat state is smooth and that, in the noninteracting approximation, the linear susceptibility does not depend on the number of excitons. To understand beating in the nonlinear regime of FWM experiments, we must deal with the fact that optical nonlinearities originate from coupling among excitons and with other sectors of the Hilbert space [19]. Given that interactions necessarily lead to lx–hx mixing or, better, to entanglement of fields, it is apparent that the few-level picture of the FWM beats gives a poor description of the wavefunction [49].

7.4. Rayleigh scattering

The picture of RRS that emerges from the theoretical results presented in section 4 is the following. Due to the disorder potential, the in-plane momentum is no longer a good quantum number and, as a result, a laser pulse of a well defined momentum couples to a continuum of exciton states with varying energies. Alternatively, the light pulse of momentum $\boldsymbol{k}_{\boldsymbol{L}||}$ couples with the exciton state of the same momentum, which then scatters into states of arbitrary momentum $\boldsymbol{q}_{||}$ because of the disorder. The amplitude for this elastic process is given by $\langle \boldsymbol{q}_{||}|\mathrm{e}^{\mathrm{i}\hat{h}_{\alpha}t/\hbar}|\boldsymbol{k}_{\boldsymbol{L}||}\rangle$. Macroscopically, only the $\boldsymbol{k}_{\boldsymbol{L}||}$ Fourier component of the electric dipole is nonzero at $t = 0$. Following scattering, light emission is observed in non-phase-matched directions as the amplitude of the associated dipole components increases with time. As shown by (22), each Fourier component of the electric dipole is a sum over a continuum of exciton modes leading to a continuum of frequencies and, thus, to decay. This is in contrast to the behaviour of the amplitudes $P_{\xi} = B_{\xi}^{+} + B_{\xi}$, which remain coherent ($\langle P_{\xi}\rangle \neq 0$ for $t \to \infty$) in the absence of inelastic scattering.

7.5. Spin coherent control

Two alternative pictures provide the framework to understand coherent control of the optical orientation. The macroscopic picture focuses on the interference between the components of the induced electric dipole, as for coherent control of the exciton density. Microscopically, assuming that only one excitonic mode (j) is involved, the state of the system after excitation by two circularly (counter-) polarized δ pulses is

$$|\Xi(t)\rangle \propto \exp[g(A_{+1,j}+\mathrm{e}^{\mathrm{i}\omega\tau}A_{-1,j})] \quad (76)$$

where g stands for all the constants; see (14). Let us write

$$A_{\pm 1,j}^{\dagger} = \frac{1}{\sqrt{2}}(A_x^{\dagger} \pm \mathrm{i}A_y^{\dagger}) \quad (77)$$

so that (76) can be expressed as

$$\exp\left[\frac{g}{\sqrt{2}}((1+\mathrm{e}^{\mathrm{i}\omega\tau})A_{x,j}^{\dagger}+\mathrm{i}(1-\mathrm{e}^{\mathrm{i}\omega\tau})A_{y,j}^{\dagger})\right] \quad (78)$$

(here, we consider circular excitation and linear detection; the other case is very similar). Then, we see that, for $\omega\tau = 2N\pi$ and $\omega\tau = 2(N+1)\pi$ where N is an integer, (78) is, respectively, a coherent state of pure x- and y-excitons. In consequence, coherent control of the linear optical orientation reflects the τ-dependent selection of the linear components (x and y). Similar arguments account for control of the circular optical orientation by means of linear excitation.

Dephasing comes into play when we consider the realistic many-mode case counterpart to (78)

$$\prod_{\xi}\exp\left[\frac{g}{\sqrt{2}}((1+\mathrm{e}^{\mathrm{i}\omega_{\xi}\tau})B_{x,\xi}^{\dagger}+\mathrm{i}(1-\mathrm{e}^{\mathrm{i}\omega_{\xi}\tau})B_{y,\xi}^{\dagger})\right] \quad (79)$$

which leads to cancellation of the overall interference, as shown in figure 4. Equation (78) provides a basis for understanding the long-time behaviour of $\mathcal{P}_l$ and $\mathcal{P}_c$, which experiments have shown to be governed by the usual spin relaxation [5]. In the single-mode case, it is not possible to distinguish between the state after excitation with one linearly polarized pulse or two delayed circularly polarized pulses with the proper delay. Hence, the same decay behaviour must apply to both cases. With minor modifications, and provided $\tau \ll T_2$, these considerations apply to the multimode situation as well.

8. Conclusions

We have presented a bosonic theory of resonantly generated QW excitons in a weak disorder potential. At low densities, the exciton state is represented by a *collective* Glauber coherent state. The picture of excitonic coherence in a perfect lattice [18] remains valid in the presence of a weak disorder potential. Although our approach delivers the same $\chi(1)$ as a 'one-exciton' approach, it highlights the idea that coherence is a many-exciton phenomena. Our results compare well with linear experiments on coherent control of the exciton density and spin [2, 5] and resonant Rayleigh scattering [3, 7–11]. We have shown that, due to the disorder, the $\boldsymbol{k}_{||}$ component of the laser field couples to all excitonic modes, including those with $\boldsymbol{q}_{||} \neq \boldsymbol{k}_{||}$. These modes re-emit light with a well defined phase relationship with the exciting laser, accounting for the observation of coherent RRS.

We have considered two types, elastic (disorder induced) and inelastic, of dephasing mechanism. Elastic processes result in decay of the induced *macroscopic* dipole in a time given by the inverse of the width associated with inhomogeneous broadening. Inelastic scattering, leading to decay of the coherence in the sense of (11), depends on the exciton density and temperature. The experimental data and, in particular, recent statistical analyses of speckle patterns [10] indicate that, at low temperatures and low excitation intensities, the inelastic-scattering time is much longer than that due to disorder.

We have discussed at length the question of the nature of the interference responsible for lx–hx beats and coherent control. In general, excitonic interferences are much closer to those of classical electrodynamics than to quantum atomic interferences. Our formalism accounts for the crossover between the quantum limit, in which only a few excitons exist in the sample, and the near-classical range that occurs under standard excitation conditions. We have introduced the concepts of macroscopic and microscopic coherent control, which correspond, respectively, to these classical and quantum limits. Macroscopic control applies to excitons, phonons [43], polaritons [44] and other extended bosonic excitations while microscopic control focuses on atomic-like systems such as quantum dots [46].

We conclude by referring to possible extensions and improvements of this work. First, a less phenomenological treatment of the problem of a single exciton in a disorder potential is desirable [25, 33]. Effects due to inter-well coupling remain to be studied. It should not be very difficult to adapt our theory to the case of a QW inside a microcavity. Transient experiments on such a system have recently been reported in [44, 50].

Acknowledgments

This work was supported by MEC of Spain under contract PB96-0085, the Fundación Ramón Areces and the US Army Research Office under contract no DAAH04-96-1-0183. One of us (JFR) wishes to thank S Haacke, B Deveaud, N Garro, R Phillips, F Sols, J S Cañizares, T Amand, X Marie and M Wörner for stimulating conversations. RM acknowledges countless discussions with D G Steel and collaborators, particularly, H Huang and N Bonadeo.

Appendix A. RRS is coherent

In this appendix, we calculate the quantum state of the light modes associated with RRS by solving exactly the problem of photons coupled to the electric dipole of the excitons and taking into account disorder. We neglect the quantum fluctuations of the induced dipole. That is, we replace the operator by its mean value, which is nonzero in the case of a disordered QW excited by a laser pulse. Hence, we need to solve

$$\mathcal{H} = \sum_{\boldsymbol{k},\lambda} \hbar c|\boldsymbol{k}| b^{\dagger}_{\boldsymbol{k},\lambda} b_{\boldsymbol{k},\lambda} - \sum_{\boldsymbol{k}_{||},k_z,\boldsymbol{\lambda},M} \mathcal{F}_{\boldsymbol{k}_{||},k_z,\boldsymbol{\lambda},M}(t)(b_{\boldsymbol{k}_{||},k_z\lambda} + \text{c.c.}) \tag{A.1}$$

where $\mathcal{F}_{\boldsymbol{k}_{||},k_z,\lambda,M}(t)$ is given by

$$\sqrt{\left(\frac{\hbar c|k|}{2\epsilon_0 V}\right)}(\hat{P}^{(+)}_{\boldsymbol{k}_{||},M} + \text{h.c.})\vec{u}_M \cdot \vec{\epsilon}_{\boldsymbol{k},\lambda}. \tag{A.2}$$

Equation (A.1) is again a problem of harmonic oscillators driven by a classical source. Note that the roles of photons and excitons are now reversed compared to the calculations of the exciton collective state, where we neglected laser fluctuations. We assume that all the $\boldsymbol{q} \neq \boldsymbol{k}_L$ photon modes are empty at $t = -\infty$. Neglecting the dipole fluctuations, the state describing the field emitted by the non-phase-matched modes is

$$|\Psi(t)\rangle \equiv S\mathrm{e}^{-\mathrm{i}H_{\mathrm{rad}}t/\hbar} \prod_{\boldsymbol{k},\alpha,M} \mathrm{e}^{\mathrm{i}\mathcal{K}_{k,\alpha,M}(t)b^{\dagger}_{k,\alpha,M}}|0\rangle \tag{A.3}$$

where S is a normalization constant and

$$\mathcal{K}_{k,\alpha,M}(t) = \frac{1}{2\hbar}\int_{-\infty}^{t} \langle \mathcal{F}_{\boldsymbol{k}_{||},k_z,\boldsymbol{\lambda},M}(s)\rangle \mathrm{e}^{\mathrm{i}cqs}\,\mathrm{d}s. \tag{A.4}$$

It follows that the quantum state of the photon field is a *coherent state*. One of the important properties of this state is that the mean value of the electric field is nonzero [15], as we showed in section 4. The light emitted by an exciton condensate has also this property [26].

Appendix B. Electric field due to coherent excitons

Here, we discuss the approximations that lead to equation (49):

$$\hat{\boldsymbol{E}}^{(+)}(z,t) = \frac{\hbar\omega^2}{16\pi^2\epsilon_0 cz}\hat{\boldsymbol{P}}^{(-)}\left(t-\frac{z}{c}\right). \tag{B.1}$$

First, we assume that $\hat{P}^{(-)}_{\boldsymbol{k}_{||}}$ is independent of $\boldsymbol{k}_{||}$ in non-phase-matched directions. This is the case of our ansätze (32) and (35). With this approximation, (46) can be written as

$$\langle\hat{\boldsymbol{E}}^{(+)}(\boldsymbol{r},t)\rangle \equiv \int_0^t \sum_M \langle\hat{P}^{(-)}_M(t')\rangle\,\mathrm{d}t' \times\left(\frac{\hbar c|k|}{2\epsilon_0 V}\right)\sum_{\boldsymbol{k}_{||},k_z,\lambda}(\vec{u}_M\cdot\vec{\epsilon}_{\lambda,\boldsymbol{k}})\vec{\epsilon}_{\lambda,\boldsymbol{k}}\mathrm{e}^{\mathrm{i}\boldsymbol{k}\cdot\boldsymbol{r}}\mathrm{e}^{\mathrm{i}c|\boldsymbol{k}|(t'-t)}. \tag{B.2}$$

We integrate using cylindrical variables with $\boldsymbol{k}\equiv k\vec{u}_k$ and

$$\begin{aligned}\vec{u}_k &= \sin(\theta)\cos(\phi)\vec{u}_x + \mathrm{sen}(\theta)\sin(\phi)\vec{u}_y + \cos(\theta)\vec{u}_z\\ \vec{u}_\theta &= \cos(\theta)\cos(\phi)\vec{u}_x + \cos(\theta)\sin(\phi)\vec{u}_y - \sin(\theta)\vec{u}_z\\ \vec{u}_\phi &= -\sin(\phi)\vec{u}_x + \cos(\phi)\vec{u}_y.\end{aligned} \tag{B.3}$$

Further $\vec{\epsilon}_{\boldsymbol{k},\lambda=1}\equiv\vec{u}_\theta$, $\vec{\epsilon}_{\boldsymbol{k},\lambda=2}\equiv\vec{u}_\phi$ and

$$\vec{u}_{M=\pm1} = \frac{1}{\sqrt{2}}(\vec{u}_x \pm \mathrm{i}\vec{u}_y). \tag{B.4}$$

The detector is placed at $\boldsymbol{r}=(0,0,z)$. As the incident laser is a plane wave and the polarization does not depend on $\boldsymbol{k}_{||}$, the field depends only on z (note that there are no speckles). For $\lambda=1$ (the other cases are very similar) we obtain

$$\boldsymbol{E}(z,t) = \left(\frac{\hbar c}{2\epsilon_0}\right)\int_0^t\langle P_{M=\pm1}(t')\rangle\int_0^{2\pi}\mathrm{d}\phi\int_0^{\pi}\mathrm{d}\theta\,\sin(\theta) \times\int_0^\infty\frac{\mathrm{d}k}{(2\pi)^3}k^3\mathrm{e}^{\pm\mathrm{i}\phi}\mathrm{e}^{\mathrm{i}kz\cos(\theta)}\mathrm{e}^{\mathrm{i}kc(t-t')}\frac{\cos(\theta)}{\sqrt{2}} \times(\cos(\theta)\cos(\phi)\vec{u}_x + \cos(\theta)\mathrm{sen}(\phi)\vec{u}_y - \sin(\theta)\vec{u}_z). \tag{B.5}$$

After a simple integration we have

$$\boldsymbol{E}(z,t) = \left(\frac{\hbar c}{16\pi^2\epsilon_0}\right)\int_0^t\langle P_{M=\pm1}(t')\rangle\vec{u}_M\frac{1}{z}\int_0^\infty k^2 \times(\mathrm{e}^{\mathrm{i}kz}-\mathrm{e}^{-\mathrm{i}kz})\mathrm{e}^{\mathrm{i}kc(t-t')}\,\mathrm{d}k\,\mathrm{d}t'. \tag{B.6}$$

Finally, we obtain (49) by applying the standard approximation [29]

$$\int_0^\infty k^2(\mathrm{e}^{\mathrm{i}kz}-\mathrm{e}^{-\mathrm{i}kz})\mathrm{e}^{\mathrm{i}kc(t-t')}\mathrm{d}k \simeq \frac{\omega^2}{c^2}\delta\left(t-t'-\frac{z}{c}\right)$$

to (B.6), where ω is an average photon frequency.

Appendix C. Gaussian pulses

Here, we solve the integral

$$\mathcal{P}_\alpha = \int_{-\infty}^t (t-s)\mathrm{e}^{-(\Gamma_\alpha-\mathrm{i}\omega_\alpha)(t-s)}E(s)\,\mathrm{d}s \tag{C.1}$$

with $E(s)$ given by the Gaussian form (38). First, we approximate the upper integration limit by ∞, which is a good approximation for times much larger than the width of the pulse. We write

$$\mathcal{P}_\alpha \approx \mathrm{e}^{-(\Gamma_\alpha-\mathrm{i}\omega_\alpha)(t-s)}(t\mathcal{I}_\alpha - \mathcal{J}_\alpha) \tag{C.2}$$

where $\mathcal{I}_\alpha = \int_{-\infty}^\infty \mathrm{e}^{(\Gamma_\alpha-\mathrm{i}\omega_\alpha)s}E(s)\,\mathrm{d}s$ and $\mathcal{J}_\alpha = \mathrm{d}\mathcal{I}_\alpha/\mathrm{d}\Gamma_\alpha$. The replacement $x = s/T - \Gamma_\alpha/2$ gives

$$\mathcal{I}_\alpha \approx E_0 T\mathrm{e}^{\frac{\Gamma_\alpha^2T^2}{2}}\int_{-\infty}^\infty \mathrm{e}^{-x^2}\mathrm{e}^{-\mathrm{i}\omega_\alpha T(x+\frac{\Gamma_\alpha T}{2})} \times\sin\left[\Omega T\left(x+\frac{\Gamma_\alpha T}{2}\right)\right]\mathrm{d}x. \tag{C.3}$$

Thus

$$\mathcal{P}_\alpha \approx E_0 T\sqrt{\frac{\pi}{2}}\mathrm{e}^{-\mathrm{i}(\omega_\alpha-\mathrm{i}\Gamma_\alpha)t}\mathrm{e}^{\frac{\Gamma_\alpha^2T^2}{4}-\frac{T^2(\omega_\alpha-\Omega)^2}{4}} \times\mathrm{e}^{-\mathrm{i}\frac{T^2\Gamma_\alpha^2(\omega_\alpha-\Omega)}{2}}\left(t-\frac{T^2\Gamma_\alpha}{2}+\mathrm{i}\Gamma_\alpha T^2(\omega_\alpha-\Omega_\alpha)\right). \tag{C.4}$$

This expression can be simplified. If we take typical values of $T=180$ fs, $\Gamma_\alpha=0.5$ meV and $(\omega_\alpha-\Omega_\alpha)=10$ meV, we have $\Gamma_\alpha T^2(\omega_\alpha-\Omega_\alpha)=0.37$ fs and $T^2\Gamma_\alpha=0.1$ fs, so we can neglect the corresponding terms to obtain

$$\mathcal{P}_\alpha \approx E_0 T\sqrt{\frac{\pi}{2}}t\mathrm{e}^{-\mathrm{i}(\omega_\alpha-\mathrm{i}\Gamma_\alpha)t}\mathrm{e}^{-\frac{T^2(\omega_\alpha-\Omega)^2}{4}}. \tag{C.5}$$

We see that the only difference between (C.5) and the expression for the δ-pulse is the factor $\exp(-\frac{T^2(\omega_\alpha-\Omega)^2}{4})$.

References

[1] Wang H *et al* 1995 *Phys. Rev. Lett.* **74** 3065
[2] Heberle A P, Baumberg J J and Köhler K 1995 *Phys. Rev. Lett.* **75** 2598
Baumberg J J *et al* 1997 *Phys. Status Solidi* b **204** 9
[3] Haacke S *et al* 1997 *Phys. Rev. Lett.* **78** 2228
Haacke S *et al* 1998 *Trends in Optics and Photonics* vol 18, ed D Citrin (Optical Society of America) p 64
[4] Gurioli M *et al* 1997 *Phys. Rev. Lett.* **78** 3205
Ceccherini *et al* 1996 *Opt. Commun.* **132** 77
[5] Marie X *et al* 1997 *Phys. Rev. Lett.* **79** 3222
Le Jeune P *et al* 1997 *Phys. Status Solidi* a **164** 527
[6] Baumberg J J *et al* 1998 *Phys. Rev. Lett.* **80** 3567
[7] Birkedal D and Shah J 1998 *Phys. Rev. Lett.* **81** 2372
[8] Wörner M and Shah J 1998 *Phys. Rev. Lett.* **81** 4208
[9] Garro N *et al* 1999 *Phys. Rev.* B **60** 4497
[10] Langbein W, Hvam J and Zimmermann R 1999 *Phys. Rev. Lett.* **82** 1040
[11] Haacke S *et al* 2000 *Phys. Rev.* B **61** R5109
[12] Shchegrov A V, Birkedal D and Shah J 1999 *Phys. Rev. Lett.* **83** 1391
[13] Stolz H 1994 *Time-Resolved Light Scattering from Excitons* (Berlin: Springer)
[14] Lang I G, Belitsky V I and Cardona M 1997 *Phys. Status Solidi* a **164** 307
[15] Glauber R J 1963 *Phys. Rev.* **131** 2766
[16] Shah J 1996 *Ultrafast Spectroscopy of Semiconductors and Semiconductor Nanostructures* (Berlin: Springer)
[17] Zimmermann R 1995 *Il Nuovo Cimento* D **17** 1801
[18] Fernandez-Rossier J, Tejedor C and Merlin R 1999 *J. Phys.: Condens. Matter* **11** 6013
Fernandez-Rossier J, Tejedor C and Merlin R 1999 *Solid State Commun.* **112** 597
[19] Victor K, Axt V M and Stahl A 1995 *Phys. Rev.* B **51** 14 164
[20] Keldysh L V and Kozlov A N 1968 *Zh. Eksp. Teor. Fiz.* **54** 978 (Engl. Transl. 1968 *Sov. Phys.–JETP* **27** 521)

[21] Schmitt-Rink S and Chemla D S 1986 *Phys. Rev. Lett.* **57** 2752
Schmitt-Rink S, Chemla D S and Miller D A B 1989 *Adv. Phys.* **38** 89
[22] Hanamura E and Haug H 1977 *Phys. Rep.* C **33** 209
[23] Citrin D 1996 *Phys. Rev.* B **54** 14 752
[24] Mandel L and Wolf E 1995 *Optical Coherence and Quantum Optics* (Cambridge: Cambridge University Press)
[25] Savona V and Zimmermmann R 1999 *Phys. Rev.* B **60** 4928
[26] Fernández-Rossier J, Tejedor C and Merlin R 1998 *Solid State Commun.* **108** 473
[27] Cohen-Tannoudji C, Dupont-Roc J and Grynberg G 1992 *Atom–Photon Interactions* (New York: Wiley)
[28] Lauterborn W, Kurz T and Wiesenfeldt M 1993 *Coherent Optics* (Berlin: Springer)
[29] Scully M and Suhail Zubairy M 1996 *Quantum Optics* (Cambridge: Cambridge University Press)
[30] Anderson P W 1984 *Basic Notions of Condensed Matter Physics* (Menlo Park: Benjamin-Cummings)
[31] Galindo A and Pascual P 1991 *Quantum Mechanics* (Berlin: Springer)
[32] Dicke R H 1954 *Phys. Rev.* **93** 99
[33] Glutsch S and Bechstedt F 1994 *Phys. Rev.* B **50** 7733
Glutsch S, Chemla D S and Bechstedt F 1996 *Phys. Rev.* B **54** 11 592
[34] Kira M, Jankhe F and Koch S W 1999 *Phys. Rev. Lett.* **82** 3544
Fernandez-Rossier J *et al* 2000 *Phys. Rev. Lett.* **84** 2281
[35] Garro N Private communication
[36] Birkedal D, Shah J and Pfeiffer L N 1999 *QUELS 99 Technical Digest* p 151
[37] Lambert L W, Compaan A and Abella I D 1971 *Phys. Rev.* A **4** 2022
Yajima T and Taira Y 1979 *J. Phys. Soc. Japan* **47** 1620
[38] Sham L J, Östreich Th and Schonhammer K 1998 *Physica* E **2** 388
[39] Damen T C *et al* 1991 *Phys. Rev. Lett.* **67** 3432
Maialle M Z, de Andrada e Silva E A and Sham L J 1993 *Phys. Rev.* B **47** 15 576
Amand T *et al* 1996 *Solid State Commun.* **100** 445
Snoke D *et al* 1997 *Phys. Rev.* B **55** 13 789
[40] Awschalon D and Kikkawa J M 1999 *Phys. Today* **52** 33
[41] Bott K *et al* 1996 *J. Opt. Soc. Am.* B **13** 1026
[42] See e.g. Gammon D *et al* 1996 *Science* **273** 87
Gammon D *et al* 1995 *Phys. Rev.* B **51** 16 785 and references therein
[43] Hase M, Itano T, Mizoguchi K and Nakashima S 1998 *Japan. J. Appl. Phys.* **37** L281
[44] Marie X *et al* 1999 *Phys. Rev.* B **59** R2494
[45] Jones R R, Raman C S, Schumacher D W and Bucksbaum P H 1993 *Phys. Rev. Lett.* **71** 2575
[46] Bonadeo N H *et al* 1998 *Science* **282** 1473
[47] Ramsey N F 1956 *Molecular Beams* (London: Oxford University Press)
[48] Haroche S 1976 *High Resolution Laser Spectroscopy* ed K Shimoda (Berlin: Springer) p 253
[49] Koch M *et al* 1992 *Phys. Rev. Lett.* **69** 3631
Zhu X, Hybertsen M S and Littlewood P B 1994 *Phys. Rev. Lett.* **73** 209
Lyssenko V G *et al* 1993 *Phys. Rev.* B **48** 5720
[50] Hayes G R *et al* 1998 *Phys. Rev.* B **58** 10 175